REPORT DOCUMENTATION PAGE	Form Approved OMB No. 0704-0188

1. AGENCY USE ONLY *(Leave blank)*	2. REPORT DATE	3. REPORT TYPE AND DATES COVERED
	13 Feb 98	

4. TITLE AND SUBTITLE
LOW TEMPERATURE SYNTHESIS AND CHARACTERIZATION OF NEW VANADIUM OXIDES

5. FUNDING NUMBERS

6. AUTHOR(S)
CURTIS L. WEEKS

7. PERFORMING ORGANIZATION NAME(S) AND ADDRESS(ES)
BINGHAMTON UNIVERSITY
STATE UNIVERSITY OF NEW YORK

8. PERFORMING ORGANIZATION REPORT NUMBER
97-165

9. SPONSORING/MONITORING AGENCY NAME(S) AND ADDRESS(ES)
THE DEPARTMENT OF THE AIR FORCE
AFIT/CIA, BLDG 125
2950 P STREET
WPAFB OH 45433

10. SPONSORING/MONITORING AGENCY REPORT NUMBER

11. SUPPLEMENTARY NOTES

12a. DISTRIBUTION AVAILABILITY STATEMENT
Unlimited Distribution
In Accordance With AFI 35-205/AFIT Sup 1

12b. DISTRIBUTION CODE

13. ABSTRACT *(Maximum 200 words)*

14. SUBJECT TERMS	15. NUMBER OF PAGES 98
	16. PRICE CODE

17. SECURITY CLASSIFICATION OF REPORT	18. SECURITY CLASSIFICATION OF THIS PAGE	19. SECURITY CLASSIFICATION OF ABSTRACT	20. LIMITATION OF ABSTRACT

LOW TEMPERATURE SYNTHESIS AND CHARACTERIZATION OF NEW VANADIUM OXIDES

BY

2LT. CURTIS L. WEEKS

BS Western New England College 1996

THESIS

Submitted in partial fulfillment of the requirements for
the degree of Master of Science in Materials Chemistry
in the Graduate School
Binghamton University
State University of New York
1997

Accepted in partial fulfillment of the requirements for
the degree of Master of Science in Materials Chemistry
in the Graduate School
Binghamton University
State University of New York
1997

M. Stanley Whittingham _____ December 12, 1997
Chemistry Department, Advisor

David Doetschman _____ December 12, 1997
Chemistry Department, Chair

Wayne Jones _____ December 12, 1997
Chemistry Department

Abstract

Transition metal oxides are receiving a great deal of attention because the materials produced are showing promise in the fields of catalysis and electrochemistry. These materials are being produced in a variety of ways, but the low temperature hydrothermal method is producing materials with desired structural characteristics.

This study discusses efforts in mild reaction conditions of heat temperatures ranging between 160 and 200 °C. The factors of pH, reaction time, reaction temperature, and the presence of organic templating cations are also studied to see their impact on traditional and microwave reactions. The relatively new field of microwave synthesis has shown that materials which customarily took 2 days of reaction time in the traditional ovens are reproducible in 30-60 minutes via the microwave ovens.

The influence of the organic cations in the reaction mediums is the focus of this particular study. The ability to produce layered vanadium oxides in the absence of such templating cations as TMA would make the materials potentially better for electrochemical purposes. This research used a variety of solvents in an attempt to produce interlayer bridging by organic anions. The solvents of ethylene glycol and acetic acid act as those bridges, each with 2 accessible oxygens.

Dedication

The time and energy that I have expended, here at this institution, I have done such for the needs of the Air Force. Those needs of the Air Force have been instilled in me by the Commandant of Cadets at my ROTC Detachment at the University of Massachusetts in Amherst. The Air Force was offered to me as a family. A family with pillars of dedication, vigor, and a desire to be part of the world's most respected Air and Space Force.

I offer this, my work, as humble tribute to a person who exemplifies the ideals of the United States Air Force. A man who's guidance and support qualified me to be a commissioned officer. His efforts in leadership education and his sacrifice of personal time to not only train, but mold cadets as good people, has focused my perception of what a patriot, a leader, and a virtuous man is. He balances a family which he overtly displays his love for, with a career that he excels at. This officer, to whom I owe so much, is Maj. John Trainor. Thank you sir for your unyielding support!

A Special Note of Thanks

-to the USAF for their benevolence in allowing me the opportunity to participate in this AFIT sponsored program. In that group of military personal who have championed my cause and career endeavors, a special thank you to: AFROTC Det. 370 UMASS Amherst, Lt. Col. F.X. Baryza (Ret.), Maj. Ross E. Dueber (Ret.), Maj. F. Conejo, Maj. R. Tolle, Maj. A. Mattera, 1Lt. G. Tolmoff, 1Lt. Roberts, 2Lt. R. Longley, 2Lt, E. Fernald, 2Lt. P. Mancinelli, and Sean Horgan.

-to home town families that have helped shaped my life so as to be Air Force officer quality: Mr. and Mrs. Hosier, Aunt Jamie and Uncle Lew, Mr. and Mrs. Uhl, Ms Keihn-Kirkey, Mr. and Mrs. Rohrlack, Mr. and Mrs. Bellino, Mr. and Mrs. Sexton. My close personal friends who kept me clean: Gys, Tom, Bill, Jim, Shawn, Mark, Kerstin, Chris, Jen, Mike, and Jean.

-to a friend who's support was without bound and never allowed me to forget my goals, thank you for everything Betty!

-to my support network in Springfield: Mike and Melissa, you have been there as friends urging my success as an officer and a chemist, (you also never let me forget that I need to play sometimes too). Friends like you are rare finds. Ted, Andy, Tara, John, Kelley, and the many other (Chiefs/triangle heads) at SC, you have all made me smile. For that, I owe you all a big thanks. The little things keep use sane and happy.

-to those at WNEC who aided me in my aspirations: Mr. Wozniak, Dr. Ball, Dr. Gajnos, Dr. Poirot, Dr. N. Hoar, Sra. Garabedian, Scott, Rich, Aaron, Leanne, Heather, Penny, Jim, Alicia, Rich, Keith, Mary, Heidi, and Dave.

-to family and friends in the Binghamton area and my local parish: our beliefs teach us that our successes are attributed to our strong faith. That strength of faith, I believe, is founded in the character of our worshiping community. Thank you all. Aunt Rita, Uncle Gene, and Christine, having close family through this academic process has been a blessing. I appreciate all that you have done to aid my endeavors.

-to Maj. Coddington, (Buzzy): without your generous advice when I was 16, and continuously since, I would have neither the direction nor the opportunities that I possess now. Thank you sir.

-a special note of thanks to someone who freely offered her home, family, and companionship to me. The ability to visit and relax with you, Katie, and Christine was a neat resource to have. Regina, you have helped me in so many ways, thank you so much. You are truly a wonderful person and I consider myself extremely lucky to have you as a part of my life.

-to my mother, father, and two sisters: I love you all and know that your guidance and support have gotten me to where I am today. We are a strong family that is such because of all that we accomplish together. We have taken different paths in our lives while maintaining a closeness of family, and equally as important, growing as friends. We have done so by our continued support of personal choices. With this step and degree completion I, as a member of the Weeks family, surge forward into life and the Air Force to make you proud. Thank you for everything!

-to SUNY Binghamton's outstanding science I and II faculty, staff, and researchers: Dr. Stevens, Dr. Suzuki, Dr. Jenkins, Elaine Schmitz, and Bill Blackburn.

-to the researchers that have guided my work, fixed the countless things that I broke, and shared this experience with me: Greg, Art, Gerald, Fan, Rongji, and Marc. I thank you all. A special note to you for all of your help this semester, thank you Ed!

-to those in the EPR lab and basement offices, thank you both for all of the help and companionship Denis and Dave.

-to my friend, who took me to Michigan/Canada and got me lost: your endless hours of support and guidance is greatly appreciated. Thank you Tom. Don't worry, I won't forget all that you taught me in "the other classroom" either. I will miss the fun that I had with you and Laura, take care.

-to Dr. Wayne Jones and Dr. David Doetschman, your participation in my learning through the Physical Methods course and Graduate seminar is sincerely appreciated. Your serving on my committee brings closure to my time here, thank you both.

-to Dr. Brigitte Pequernard, thank you for your efforts in the EPR and susceptibility end of my research, and the countless questions that you answered. I will miss our chats, as friends and as two culturally different people, a great deal.

-to Dr. Peter Yu. Zavalij, our university crystallographer: thank you for the energy that you gave to my materials, but also of your generosity of personal time in teaching me about crystallography.

-to the National Science Foundation for their support of our on going research at the University.

Dr. M. Stanley Whittingham- Your investment in me is unrepayable. I sincerely thank you for your attention and continued efforts in helping me meet the prescribed goals of the Air Force, and giving me the tools to grow and learn here at the University. I have both enjoyed and learned from being a part of the Materials Group and IMR. Thank you!

Table of Contents

Tables

Figures

Chapter I -Purpose

One of the focuses of our, National Science Foundation funded, program is the synthesis of new vanadium oxide materials using hydrothermal means. Many of our reactions have used templating cation molecules, like the tetramethylammonium ion (TMA), in aqueous solutions to direct the structure. My component of the research has been to explore the impact of removing this quaternary ammonium cation from the reaction mixture, and to use other solvents such as glacial acetic acid and ethylene glycol.

This research has applicability to daily use as well as in our national defense department. The potential uses of a less expensive and more effective secondary battery are without bound in the civilian community as well as in the military community. The United States Air Force, through the Air Force Institute of Technology (AFIT) has allowed me the opportunity to work with, and learn from, the Institute of Materials Research (IMR) in hopes that these more efficient and less expensive materials can be synthesized.

Chapter II - Introduction

MATERIALS RESEARCH GROUP

The reason that the Materials Research Group continues to synthesize and analyze new transition metal oxides partly lies in the transition metal's ability to have several oxidation states. A diverse range of oxidation states potentially allows for several different types of coordination to occur for the transition metal. Vanadium oxides typically exhibit oxidation states of III, IV, or V. Different materials synthesized show the vanadium atoms in various coordination sites, such as tetrahedral, square pyramidal, trigonal bipyramidal, and octahedral. Because vanadium occupies an array of coordinations in oxide polyhedra, vanadium oxide materials have been shown to comprise one dimensional chain structures, as well as the multidimensional cluster, cage, tunnel, and open layered structures. These dimensions are represented in figure 1i.

The ability to synthesize layered materials, which can act as hosts for cation intercalation, is what makes vanadium oxides potentially good cathodes for secondary (rechargeable) batteries. The Materials Research Group works with the small and very electropositive lithium ions. Highly crystalline solids are a desired synthesis product for the lithium ion intercalation. Current research also shows some support that amorphous materials may be useful as cathode material.[1] The materials which are viewed to be good are those that can intercalate lithium in a 1:1 molar ratio of Li^+ to transition metal with a voltage of about 3.5V in a lithium cell. Whittingham (et. al.), in a publication about solid electrodes,[2] describe four attributes of good solid cathodes:

1-dimensional chains, ribbons

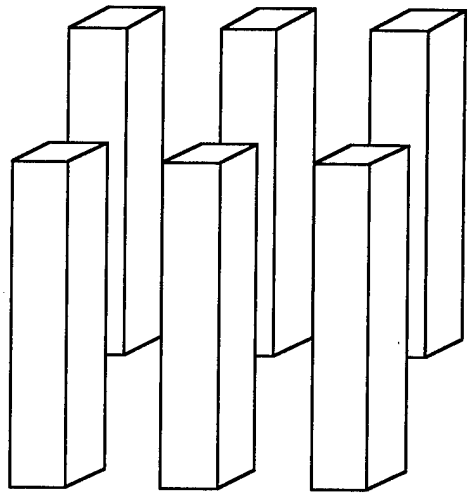

2-dimensional layers, sheets

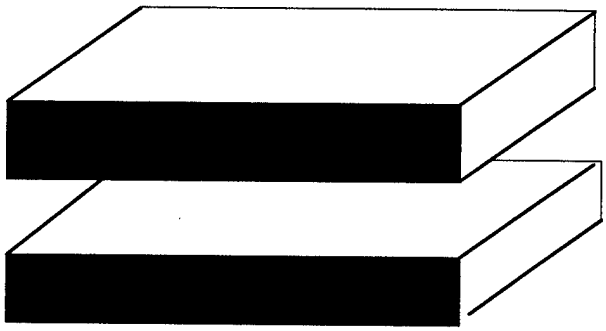

3-dimensional tunnels

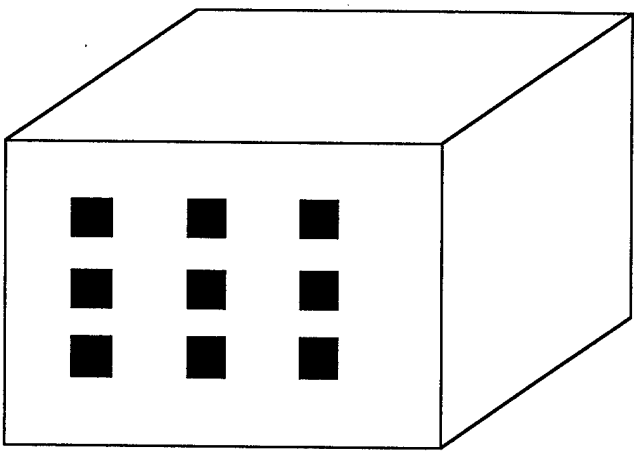

Figure 1i. Different dimensional structures formed from vanadium oxide polyhedra.

1. A high free energy of reaction with lithium; this equates to 1 Li reacting per transition metal, and a cell voltage of 3.0-3.5V.
2. Rapid reaction with lithium to give a high power density. Electrochemically this equates to a rate of 10 mA cm^{-2}. [3]
3. Complete chemical reversibility, which is almost always attained if the crystalline structure does not change during reaction lithium.
4. Low cost and low toxicity.

HISTORY OF TRANSITION METAL RESEARCH

The study of transition metal oxides continues to be a productive area of secondary battery exploration after nearly three decades. This well established field is still an area rich in opportunity. The ability of the group VI elements to form layered structures with transition metals was heavily developed by Exxon in the 70's. They worked extensively in trying to understand the superconducting properties of transition metal dichalcogenides.[4] The superconducting transition temperature was subsequently raised by intercalation of lithium ions into the structures. For most of the materials, the insertion of the lithium was "proceeded by a simple expansion of the lattice at the Van der Waals gap".[4] The lithium insertion process is shown in a rather crude manner in figure 2i. Some materials that Exxon produced with lithiated counterparts had structural reorientation due to lithium intercalation when reacted with n-butyllithium. The n-butyllithium reaction was described by Dines in 1975.[5] The many transition metal chalcogenides reported at that time offered insufficient explanation of why the interlayer spacing would expand almost 3Å[6,7,8] upon Li^+ intercalation. The size of the lithium ion would justify perhaps only around 1Å increase since the ionic radius of Li is 0.69Å. It was then proposed that NH_3 was in the layers and would thus support a larger interlayer spacing than calculated for a simple Li ion intercalation.

Some of the original transition metal chalcogenides and their ratios to lithiated counterparts are listed in Table 1i. The table originates from the first reference.

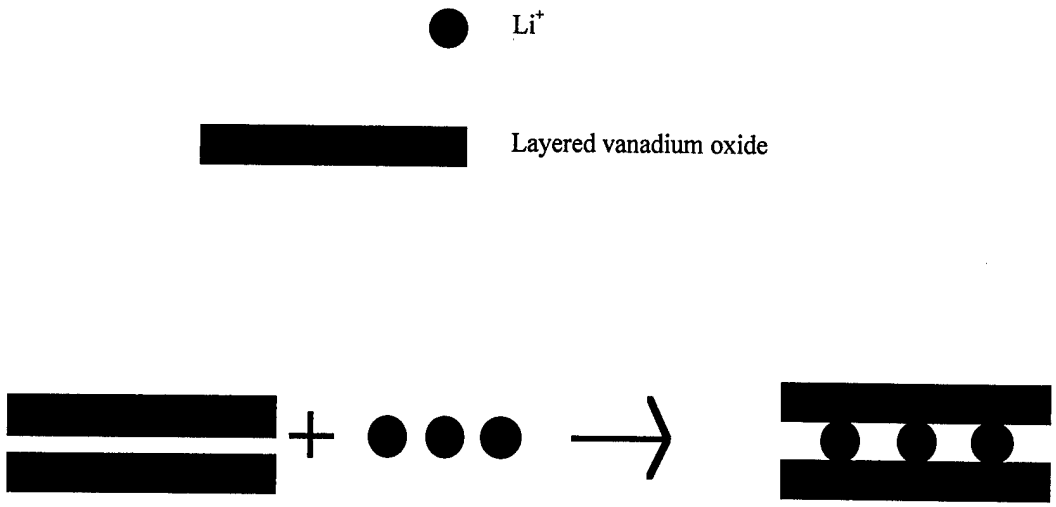

Figure 2i. The lithium insertion process into a layered vanadium oxide.

Table 1i. Exxon's list of dichalcogenides and their lithiated counterparts.[4]

X-ray Parameters of Pure and Intercalated Compounds							
	Initial			Products			
Compound	a	c	c/a	a	c	c/a	Δ C
TiS_2	3.407	1 x 5.696	1.672	3.455	1 x 6195	1.793	0.5
ZrS_2	3.665	1 x 5.835	1.592	3.604	3 x 6.25	1.734	0.42
HfS_2	3.635	1 x 5.856	1.611	3.56	3 x 6.375	1.791	0.52
NbS_2	3.34	3 x 6	1.796	3.342	3 x 6.421	1.921	0.42
TaS_2	3.34	2 x 6.04	1.808	3.34	2 x 6.475	1.939	0.44
MoS_2	3.16	2 x 6.15	1.946		? x 6.4		0.25
WS_2	3.16	2 x 6.18	1.956				
$TiSe_2$	3.535	1 x 6.004	1.698	3.644	1 x 6.48	1.778	0.48
$ZrSe_2$	3.776	1 x 6.160	1.631	3.734	1 x 6.648	1.78	0.49
$HfSe_2$	3.742	1 x 6.160	1.646	3.715	1 x 6.642	1.788	0.48
VSe_2	3.35	1 x 6.1	1.821	3.584	1 x 6.356	1.773	0.26
$NbSe_2$	3.45	2 x 6.27	1.817	3.496	2 x 6.772	1.937	0.5
$TaSe_2$	3.436	2 x 6.348	1.847	3.477	? x 6.817	1.961	0.47
$MoSe_2$	3.3	2 x 6.5	1.97				
WSe_2	3.3	2 x 6.5	1.97				

The lithium ion is used because of its: light weight, relatively low cost, and that its small size and highly electropositive charge which leads to a high cell voltage. The $LiCoO_2$ material is presently used by SONY, in their Li-ion batteries but is far too expensive for commercial use.

PREFERRED STRUCTURAL FEATURES

Open structures are preferred over close packed structures because of their ability to intercalate lithium between layers, chains, or into tunnels. Problems encountered by those working with intercalation of close packed structures reside in the difficulty of insertion and resulting structural distortion after ion insertion. The close packed lattices do not offer a tunnel, or an opening for Li ions to migrate through. They must therefore be forced into the structure. The more stable close packed structures lose their inherent stability when interstitial sites are filled, and thus the layers are spread apart. The ability to charge and discharge a battery without degradation to the structure, is of primary importance to the study of cathode materials for secondary batteries.

Preparation of materials is accomplished with anticipation that the interlayer spacing is comparable to that of the desired intercalation cation. The interlayer spacing needed for Li^+ is only 0.69Å.[9] Insertion is dependent on the material's ability to be reduced, where the insertion rate of the ion pertains to the coordination of the sites and their proximity to each other for ion transport in the metal oxide layer.

The starting materials used to produce the open structures are critical. Some compounds show little potential in attaining multidimensional structures, where others offer promising results. Persistent work with those that are promising will allow structures of the desired specifications to be produced and implemented in the growing field of battery research.

Currently a great deal of work is being conducted on manganese and vanadium in the field of electrochemical research for secondary batteries.[10,14] Currently the materials group's efforts are heavily focused on vanadium, which is readily oxidizable and frequently forms layers or sheets. V_2O_5 is the primary starting material for these reactions. This relatively inexpensive compound, has a layered structure made of square pyramids (SP). The vanadium molecules have nearly a V^{+5} oxidation state across nearly the entire sheet.[15,16] The V_2O_5 oxide contains oxygen vacancies balanced by the presence of extra electrons that allow for the existence of V^{+4} ions. It was shown previously that the unpaired electron is delocalized over the two vanadiums sites located on each side of the oxygen vacancy. In pure V_2O_5 powder, the paramagnetic defect gives a broad EPR signal with a linewidth of 85 Gauss and a g factor of 1.97. [15,16] The structure of the pentoxide is shown in figure 3i. These SP coordinated vanadium oxides are arranged in pairs. The SPs lie in such a way that the apices of two adjacent SP are pointing up, then two are pointing down, then two up again, and so on.

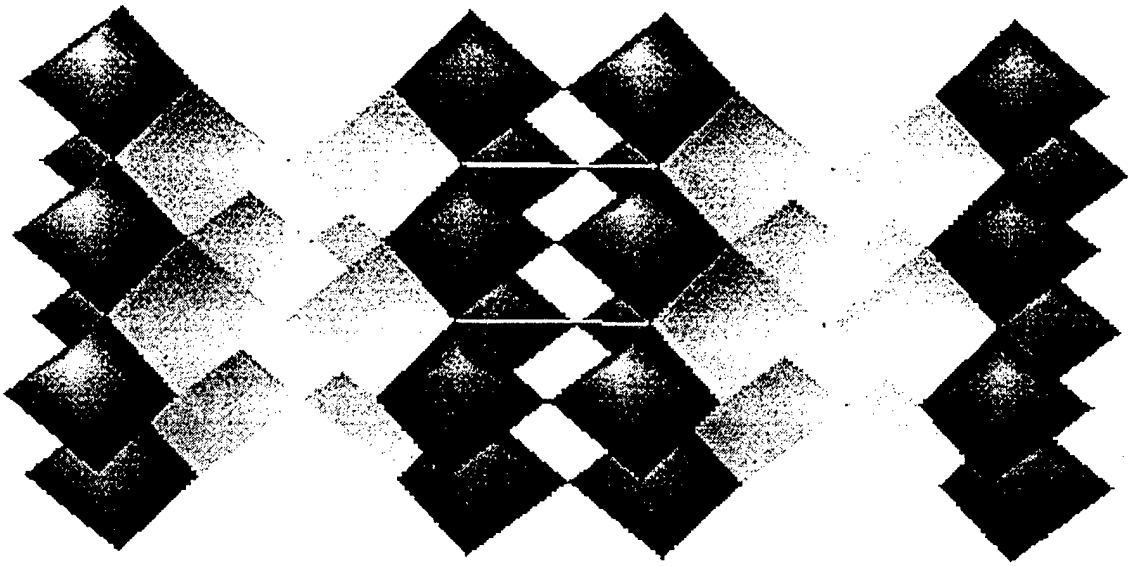

Figure 3i. The structure of V_2O_5.

STARTING MATERIALS

There has been much work done on the V_2O_5 material and its lithiated counterparts. "The Li-V_2O_5 battery system, both in active and reserve configuration, was one of the earliest battery systems developed by Honeywell for military and medical applications". [17] There are several distinct lithiated phases of pentoxide. $Li_xV_2O_5$ exists where the value of x ranges from $0 \rightarrow 3$ corresponding to the $\alpha,\varepsilon,\delta,\gamma$, and ω phases. Figure 4i depicts the most recent distinction of phases discriminated by lithium content.[16] The different phases show the importance of matching the appropriate size of the intercalated ion size to that of the site size. The quantity of the lithium intercalated is also an important feature which is studied. A large disordering is observed in the $Li_xV_2O_5$ phase where $x>1$. There has been a great deal of work on the lithiated phases, and much of that work was through EPR investigation.[18,19,20] The structures of the phases are shown in figure 5i. As mentioned earlier, a research goal is to produce materials that not only accept lithium ions in a 1:1 molar ratio with the transition metal, but also to retain structural integrity upon the cycling in a lithium cell.

The α-$Li_xV_2O_5$ phase structure exists as a slight distortion compared to the V_2O_5 lattice structure. Controversy exists as to the appropriate Li content of the different phases. For example the existence domain for the α-phase was found to be between 0.0 and 0.15 by Murphy in 1979,[21] then in 1991, Concciantelli reported the existence of the phase between 0.0 and 0.1,[22] and finally Pecquenard (et.al.) in 1995, found limits varying from 0.0 to 0.05 [15] by EPR spectroscopy. Pecquenard (et.al.) showed the prior works to

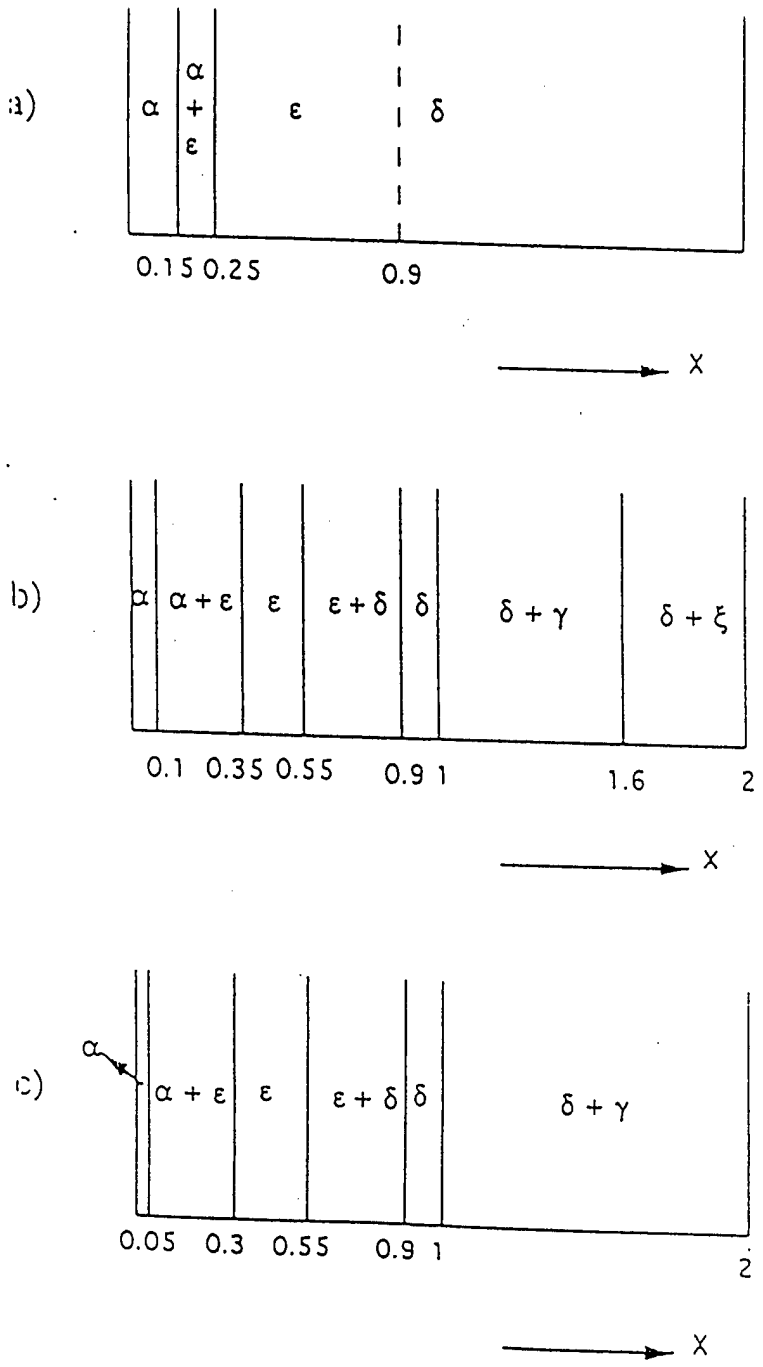

Figure 4i. The phase domains assigned by a) Murphy in 1979, b) Cocciantilli in1990, and Pecquenard in 1995.[16,21,22]

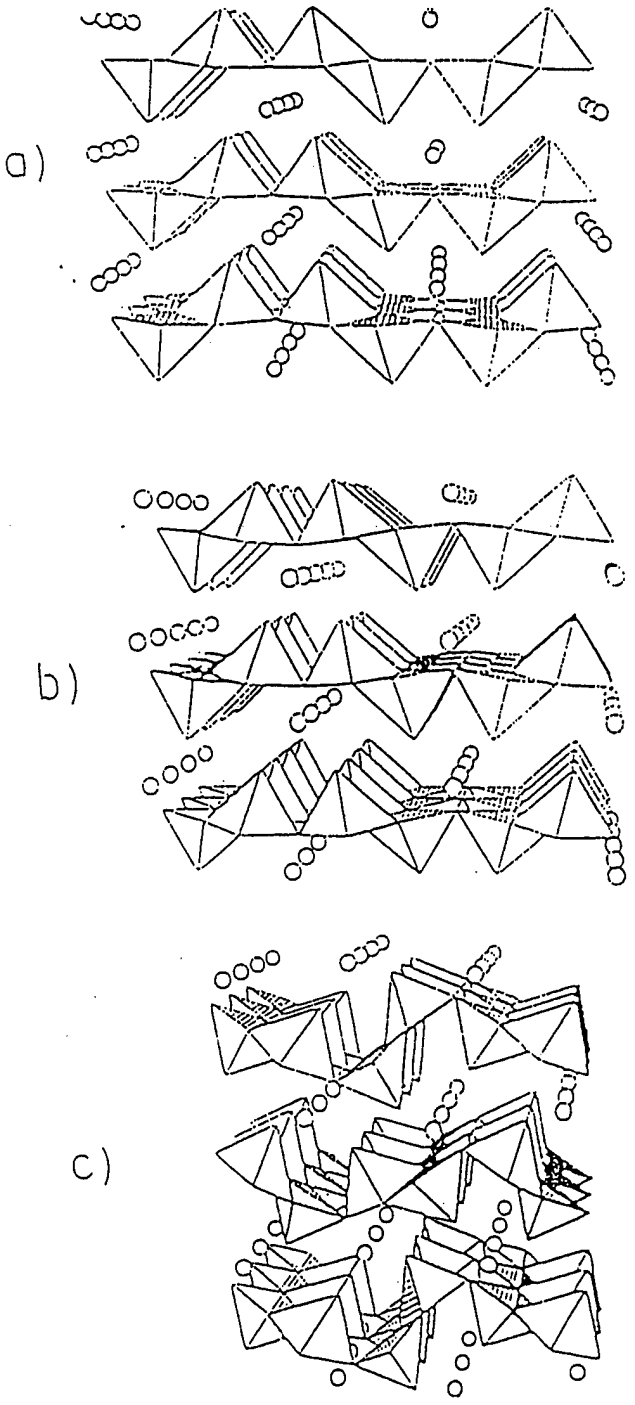

Figure 5i. The structures of $Li_xV_2O_5$ exhibiting the different degrees of puckering in the α,ε, and δ phases.[16]

be less accurate by proving that some of the epsilon phase is present from 0.05-.3.

The more puckered ε phase, where the Li content range is between 0.3 and 0.55, starts to show the limitation to the amount of the intercalated ions. The δ phase exhibits a major puckering of the pentoxide layers when there is between 0.9 and 1.0 ions in the sheets. A severe distortion exists when the Li content is greater than 2 ions per V_2O_5. The structure is not only more puckered, but a rearranging of the vanadium SP also occurs. The framework that shows the pairs of apices pointing in the same direction no longer exists with $x \geq 2$. It exhibits an alternating arrangement of apices of one up and then one down, and so on in the γ phase.

Figure 6i describes the different phases that come about during the cycling of V_2O_5 as a function of the lithium content. [16]

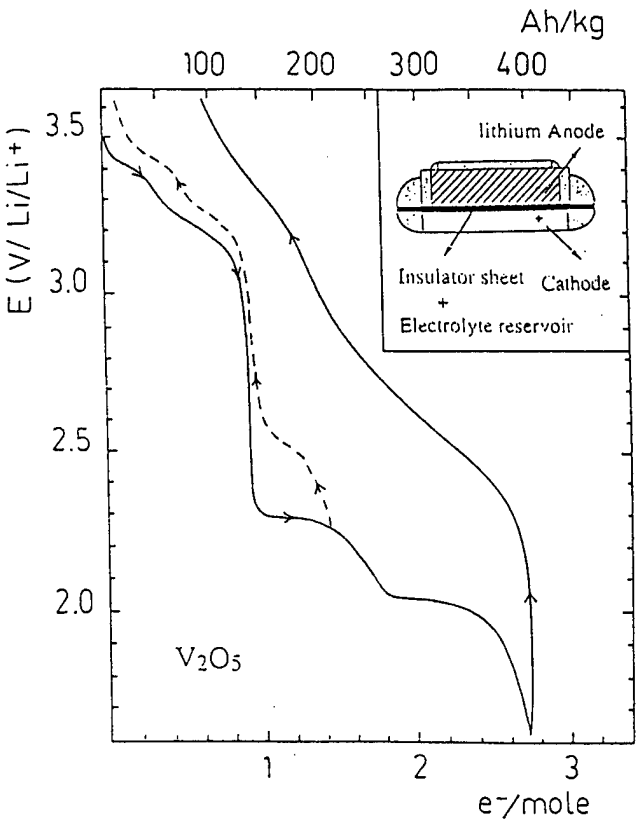

Figure 6i. A cycling plot for V_2O_5 showing its phase transition.

REACTIONS

The vanadium oxide sheets, favorably, demonstrate a characteristic net negative charge. That negative charge is what attracts the addition of organic cations in the reaction medium. Organic cations are presently being used to direct structure. The organic cations are thought to be both templating as well as structurally supportive in the vanadium oxide layers. The templating behavior is a location or a site in the reaction medium where the oxide layers form around the ions. Organic cations such as the tetramethylammonmium ion (TMA), methylamine, and ethylenediamine(en-) are presently being explored in the structure directing role.

The low temperature hydrothermal technique has been shown to be a preferred method for the syntheses of these metastable compounds. The exploration of these new vanadium oxides has occurred in both traditional and microwave reaction vessels. The two techniques both yield positive results. Chirayil (et al.) described the history of the hydrothermal reactions as having been "extensively employed for the synthesis of zeolites and metal phosphates,[23-26] but only recently have transition metal oxides been formed". [27,28]

Limitations of high temperature solid state synthesis has led to the research in utilization of a low temperature method that applied a soft chemical reaction method. According to Cheetham and Day "much solid state chemistry is lost at these high temperatures".[29] They wrote of the importance of mass transport or diffusion of solid particles, and how high temperature methods increase their rates. They further noted the

pioneer the use of microwave synthesis as a viable option. His production of titanium phosphate powders and Girnus' single crystal zeolites, both made in less than an hour, led to testing this technique in the field of the transition metal oxides. [32]

There are several advantages in using the microwave's rapid reaction time with the speed of reproduction being the most important. The method, unfortunately, has not yet allowed for the synthesis of all materials that can be produced in traditional ovens. The samples in the microwave are brought to the programmed reaction temperature in five minutes, whereas it takes two hours for the traditional oven sample to reach the desired temperatures. That rapid temperature change may be a contributing factor discriminating against the formation of some materials. More work in that area is needed to fully understand the microwave process.

REACTIONS WITH TMA

The hydrothermal synthesis of new compounds is proving to be a fruitful technique for producing new transition metal oxides.[27] This technique often yields metastable, open, or layered compounds. In the case of vanadium oxide, five new compounds have been formed simply by changing the pH of the reaction medium.[33] In that study, the pH was buffered by the use of (weak) 3M acetic acid in the presence of tetramethylammonium ions. In most cases, the tetramethylammonium ions are incorporated between vanadium oxide extended sheets giving the compositions $TMAV_3O_7$, $TMAV_4O_{10}$, $TMA_{1.2}V_8O_{20}$ and $TMA_{0.17}V_2O_5$ as the pH is reduced from 8 to 2.6.[28,33,34,35] The coordination around the vanadium increases from 4 to 6 through this series of compounds.

In the vast array of the work in the area, Chirayil (et. al.) has shown that the new layered phase of $Li_{0.6}V_{2-\delta}O_{4-\delta}$ could not be formed in the absence of the TMA ion, however there was no TMA present in the final precipitate.[35,36]

Figure 7i. $TMAV_3O_7$, a layered vanadium oxide, showing structural support by the presence of the TMA ions.

MY RESEARCH COMPONENT

The extensive work being done on the use of the organic cation has led to this specific research. Structures formed in the presence of organic cations are multidimensional but often display modest electrochemical results. The organic ions, such as TMA^+, are site inhibiting to the Li ions, because their bulky presence restricts the amount of intercalation. The layered $TMAV_3O_7$ compound, for example, would be more applicable for electrochemical purposes if the TMA was to be removed and the material maintain a layered structure. This work explored the impact of using these mild hydrothermal techniques in the absence of organic cations. This research was initiated not only to explore the necessity an organic cation in the formation of layered compounds, but also to generate new and potentially useful oxides.

In the pursuit of new and useful solid materials, much effort is spent in their characterization. The ability to resolve structures and characterize their properties quickly and effectively is what prescribes the instrumentation used. Research in the Materials Research group relies heavily upon the use of powder X-ray diffraction. This technique "provides a convenient and characteristic fingerprint which can be used in analysis. The most definite structural data has largely been acquired using diffraction methods". [25] Coupled to the X-ray powder diffraction are the analytical probes of thermalgravimetric measurements, FTIR studies, and electrochemical interrogation of the materials. These probes are significant in the determination of a material's composition, and are frequently used to substantiate the presence of organics and the proposed bonding. Since the results from the X-ray diffraction data are rapid and profitable, many

of the aforementioned analytical probes are used as resources to reinforce the crystallographic results.

Chapter III - Experimental

SYNTHESIS

Hydrothermal syntheses are the primary means of sample preparation in the materials group. Two different types of hydrothermal reactions explored in this study. They use traditional and microwave ovens for heating. The hydrothermal, or solvothermal, process utilizes the interaction of the reaction mixture in the liquid and often vapor phase. The reaction mixtures are frequently heated to a temperature above the solvent's boiling point. The products then precipitate out of the vapor and liquid phases in the reaction vessel. The variables, affecting the product formation, that are studied include: heat temperature, heat time, pH, and the use of templating ions.

The sample preparations for both oven methods are extremely similar. The quantity of the reactants used is the primary difference which is due to the smaller volumetric capacity of the microwave vessels. The traditional vessels are Teflon coated vessels encased in steel Parr autoclaves (bombs), as shown in figure 1x. Two sizes, 50mL and 125mL, of the traditional vessels were used. (They are sized by the volume capabilities of the Teflon liners.) The recommendation, by the Parr company, is not to fill the vessels any more than 1/2 to 2/3 full with the reactant mixture.

The microwave vessels were comparable in size to the smaller 50mL Parr vessels. The company producing the microwave vessels recommend only a filling of 1/3 of the vessel's capacity.

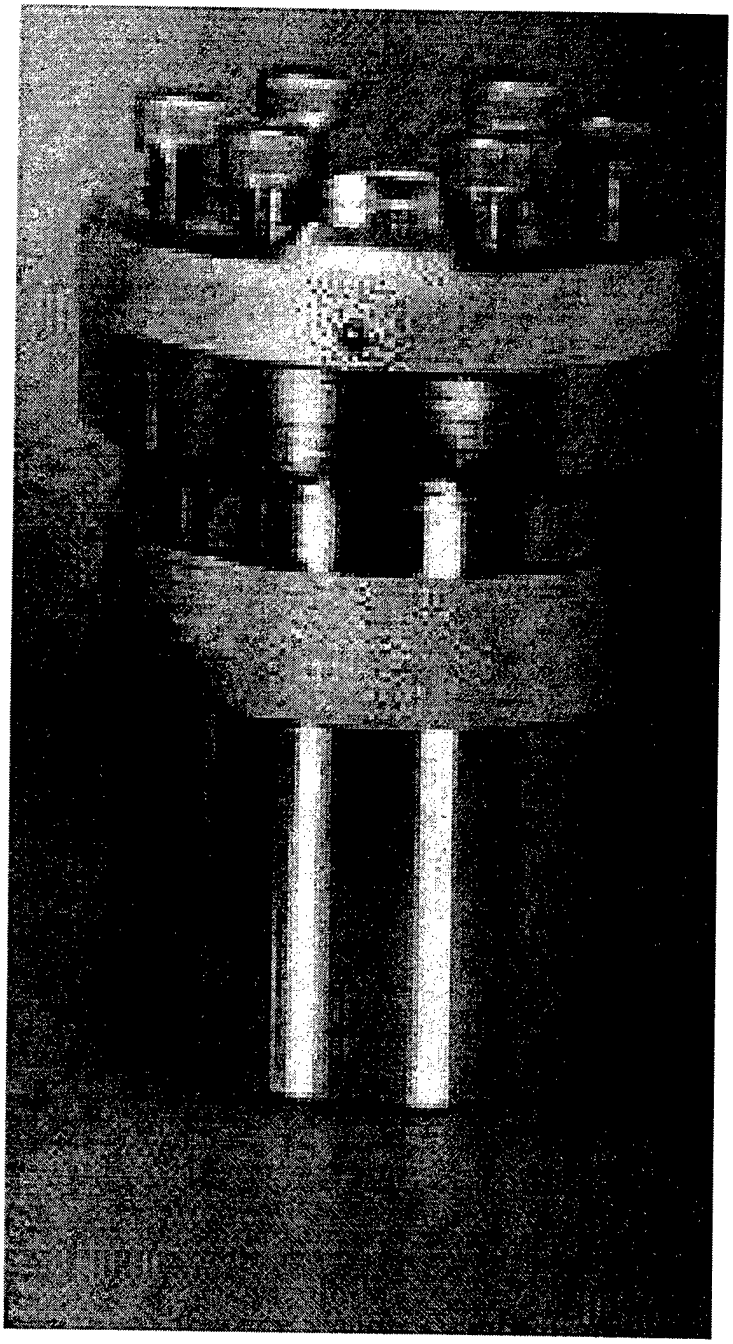

Figure 1x. Parr reaction vessel. (Steel Autoclave/Bomb)

The following is a general format of the synthesis preparation and characterization procedures. Also included is a description of the instrumentation used throughout the research. Depending on the materials used and subsequently different products formed, the procedure varied slightly. Those variations will be noted in the descriptions specific to each compound at the end of the experimental chapter.

The reactant mixtures were made in a systematic fashion for both hydrothermal types. The preparation started with weighing out the solids V_2O_5 and LiOH (when used). The samples were then poured into beakers followed by the solvents. The primary solvents of: distilled water, ethylene glycol, glacial acetic acid, 1M lithium hydroxide, and 3M acetic acid, were all used throughout the reactions. V_2O_5 is weakly acidic and only slightly soluble in the glacial acetic acid and glycol solvents, undissolved V_2O_5 persisted in the preparation beakers. The residual solid was then poured into the reaction container. (Reactions run where the solid was not added demonstrated no significant change in the products formed during reaction.)

The different methods for preparation, consisting of variations in: molar ratios, temperatures, heating conditions, pH, and solvent choice, of the A,B,C,E,F, and sol-gel materials are displayed later in table 1x.

To determine the cumulative results of starting with differing degrees of homogeneity in the mixture, the stir time was varied from 15 minutes and 12 days for the samples before heating. It was soon learned that the homogeneity was not an integral part of the reaction process. Thus, from that point the stir time corresponded to only the convenience of the researcher.

The pH of the solution was measured prior to synthesis, and in some cases the pH was adjusted by the addition of 3M acetic acid. With the pH measured, or the desired level attained, the samples were then poured into their respective hydrothermal vessels.

For the vast majority of reactions the ovens, both traditional and microwave, were set at a temperature of 200°C. The traditional oven method includes the use of a simple heating oven set at a constant temperature, and once the steel bombs are placed in the oven and the oven corrects for the loss of heat by the oven door opening, it maintains that temperature for the duration of the reaction.

The microwave oven holds a maximum of 6 vessels. The number of reaction vessels placed in the microwave oven is actually significant in the instrument's set up. The tray, that the vessels sit on, is millimeters above the bottom of the oven. Therefore, 2,3,4, or 6 vessels will keep the tray level. The oven is programmed to maintain the desired temperature while monitoring the pressure in the vessel. One of the vessels has an adapter that allows for a temperature probe to be inserted into the vessel. The probe is not in contact with the sample due to a glass casing that shields it from the reactants. The microwave vessel, with the temperature probe, also has an adapter to monitor the pressure in the system. The vessels have replaceable membranes that rupture when the pressure of the vessel exceeds its capacity. The pressure can be viewed throughout the entire reaction on a display at the top of the instrument.

Upon completion of the desired reaction time the vessels were cooled down to room temperature. The cooling process differed for the microwave and traditional ovens.

The microwave vessels were allowed to remain in the oven for 2-3 hours before being disassembled form the temperature and pressure probes. If disconnected earlier, the pressure adapt would vent the sample vapors. The traditional vessels were cooled by removing from the oven and placing them in a fume hood. They were allowed to cool for 3 hours prior to filtration.

After the synthesis, the pH of the solution containing the newly formed products, was measured again. The products were filtered and rinsed with distilled water. The thoroughly rinsed products were then placed in a drying oven, that is maintained between 45-55°C for a minimum of 3 hours. Three hours is sufficient time for most samples to dry adequately for grinding.

The chart below depicts some of the various starting compounds used to produce the materials of interest. In realizing that 30-40 trials yielded roughly the same material for several of the materials that were produced. It is not beneficial to discuss each material and their subtle differences. The best product will be thoroughly described in the extended discussion of the respective materials.

(Table 1x) The different approached investigated in the production of the 6 compounds that were produced.)

Material	V_2O_5:LiOH molar ratio	Solvent(s)	Oven types	Heat Time	pH in	pH out	Colors
A	1:2 to 1:10	ethylene glycol	trad mic	2-8 days 60 min	5.1 - 10.3	6.5 - 7.6	green blue black
B	1:1 to 2:1	ethylene glycol and acetic acid	trad mic	2-4 days 60 min	2.1 - 7	2.0 - 7	purple
C	not critical	acetic acid	trad mic	2-6 days 60 min	1.5 - 2.0	1.5 - 2.3	tan
E	no LiOH	acetic acid and distilled water	trad	2-4 days	1.7	1.6	blue black
F	no LiOH	acetic acid and distilled water	trad	4 days	2.1	2.3	green
sol-gel	.2g V_2O_5	1M LiOH and 3M acetic acid	mic	60 min	2.9 - 3.5		blue black

(Table 2x) The reagents used and manufacturer.

Starting Materials	Chemical Company
V_2O_5	Alfa
LiOH, (3M)	Fisher Scientific
Glacial Acetic Acid (17M)	Fisher Scientific
Ethylene Glycol	Aldrich

CHARACTERIZATION PROCESS

For X-ray analysis the dry products are ground with a mortar and pestle into an extremely fine powder. That fine powder is then placed onto sample holders. They are mounted with double sided tape. The samples are X-rayed in a Scintag 2000XDS θ-θ diffractometer with CuKα radiation for (λCuKα = 1.5418Å). A picture of the θ-θ diffractometer is shown in figure 2x. The data is collected in the 2θ range of 2 to 60 ° at a scan rate of 1 °2θ per second.

Thermal gravimetric analysis of the material is frequently the next step in the characterization sequence. Roughly 30 mg of material is placed in a Pt pan. (The pan is 1/4″ in diameter and roughly 3/16″ deep.) The Perkin-Elmer Model TGA 7 is programmed to heat at a scan rate of 5 °C per minute, and from 30 to 500 °C under a flow of oxygen or nitrogen gas. Oxygen flow is often used because the materials of study are readily oxidized to V_2O_5. The advantage of fully oxidizing the sample lies in the calculation of phase compositions that occur. One would use a nitrogen flow if they were interested in analyzing the reduced form of the vanadium compounds. The TGA allows for the monitoring of the weight % of the sample as a function of temperature. Using 500 °C as a maximum temperature ensures that the melting point of vanadium pentoxide is not attained.

Scintag Diffractometer

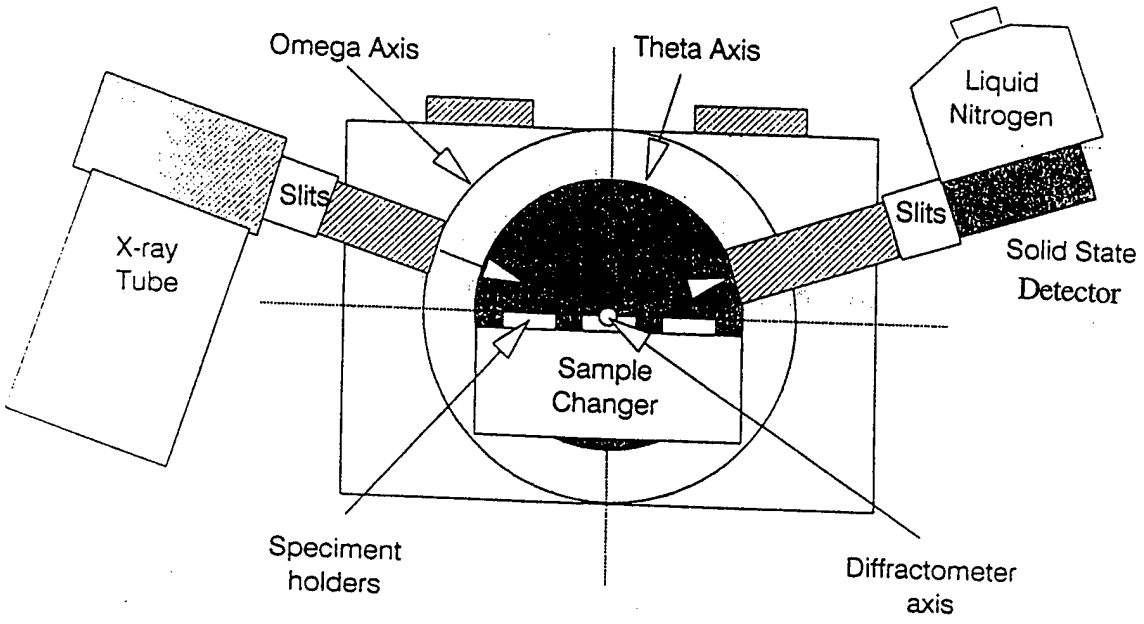

Figure 2x. The Scintag 2000XDS Diffractometer.

The Fourier Transform Infrared (FTIR) transmittance is measured from 4000 cm^{-1} to 500 cm^{-1} on a Perkin-Elmer 1600 series spectrometer. The material is well ground with KBr and pressed into a pellet.

The images of the powder were obtained using a XJD Jeol 8900 Electron Microprobe/SEM in the Geology Department at Binghamton University. The samples are sputtered with gold to avoid a charge build up on the samples and to enhances the images' resolution.

Electrochemical properties of $VO(CH_3COO)_2$ and $V_3O_7(OH_2)$ were tested in a lithium cell using an 80% weight ratio of the respective products to 10% carbon black and 10% Teflon binder. The pellet was hot pressed on a stainless steel Exmet grid at 200°C. The electrolyte used was 1M $LiAsF_6$ /propylene carbonate (PC) and Dimethoxyethane (DME) in a 1:1 volume ratio. The data was collected by a MacPile program.

Electron Paramagnetic Resonance spectra are obtained using a Bruker spectrometer. The instrument was used as a probe to establish the presence of the V^{+4} (d^1). All signals consisted of a single EPR line without resolved hyperfine structure and without resolved anisotropy of the g factor. The parallel and perpendicular turning points, characteristic of a chemical "powder" lineshape cannot be distinguished because of the existence of broad lines. The materials were only investigated at room temperature. A fine powder sample was investigated after being placed in a thin quartz tube that was filled 3/8″ high with sample.

There was a spectrum acquired for all compounds under the following standard conditions for the room temperature investigation:

Attenuation	15 dB
Power	10.31 Watts
Gain	49
Sample Weight	0.200g
Cavity Temperature	Room Temperature

Magnetic properties of the samples were also explored using a Superconducting Quantum Interference Device (SQUID) Magnetometer in the Physics Department at Binghamton University. The samples are prepared for the magnetometer by weighing, on an analytical balance accurate to a 5^{th} decimal place, a sample of roughly 50 mg, and placing it in a capsule. Due to the large temperature range of the susceptibility scan there is cotton packed into the top of the capsule to alleviate the problems caused by expansion of the material and the trapped gases upon heating during the scan. The investigation was carried out over the temperature range of 2-300 K. The applied field was maintained at a constant 1000 gauss.

COMPOUNDS SYNTHESIZED

Vanadyl Acetate : $VO(CH_2COO)_2$

Material C was made from a mixture of V_2O_5, LiOH, and glacial acetic acid. The ratio of the solids did not seem to influence the sample quality other than that some samples had a large amount of V_2O_5 that persisted after heating the vessel. When only 0.2g of V_2O_5 was in the reaction chamber there was no residual V_2O_5 after heating to 200 °C for 2 days. The preparation of the C material was also accomplished without the presence of LiOH.

The sample was made via microwave hydrothermal synthesis as well. In the microwave reactions, the addition of LiOH was essential to the formation of the vanadyl acetate, because without LiOH no reaction occurred. The pressure of the vessels, at 200°C were monitored and showed a range from 80-120PSI.

The sample was X-rayed from 10 to 90 °2θ at a scan rate of 0.02 °2θ per step and 30 seconds per point. The indexing, using the Profan program, and structure determination were successful using the CSD software.

Vanadyl Glycolate : $VO(OCH_2CH_2O)$

The B material was also produced from varied starting ratios of V_2O_5 and LiOH in 50mL of ethylene glycol. The ratio of vanadium pentoxide to lithium hydroxide was explored between 1:1 and 1:2 in the traditional oven synthesis at 200 °C. Initial pH ranged from 2.3 to 4.1, while the final was between 2.1 and 4.5. The B material was also synthesized in the microwave oven at 200 °C. The ratio of solids was again between 1:1 and 1:2. Many of the samples had their pH adjusted by the addition of 3 Molar acetic acid. With a molar ratio of 1:1 of the V_2O_5: LiOH, the pH allowable range was from 7-2.1. The initial pH was also varied for ratios other than 1:1. There was no affect of product formation when the molar ratio was changed.

The pH of the solutions produced in the bombs remained very close to the initial pH values for those adjusted with the acetic acid. That was consistent with earlier work citing the use of dilute acetic acid as a buffering agent in the mild hydrothermal method.[33]

The sample was ground into a mesh grid before being scanned from 8-90 °2θ at a rate of 0.1 °2θ per minute. That produced a pattern that was indexed using the Profran program, which led to the structure being solved. Both by using the CSD software.

$V_3O_7(OH_2)$

Material F was produced using traditional hydrothermal means. The starting materials for the compound were 0.4 g of V_2O_5, 15 mL glacial acetic acid, and 35 mL of distilled water. Heating times of 1-4 days were explored, but only the 3 and 4 days of heating at 200 °C were successful in the sample being produced. The initial and final pH values of the mixture were 2.1 and 2.3 respectively.

Production of the material via microwave hydrothermal and through varied amounts of the starting reagents, has yet to be accomplished.

The X-ray powder pattern of the sample was obtained from 2-60 °2θ at a scan rate of 1° 2θ per minute. Indexing was then accomplished using the Profan program from the CSD software and was followed by the structure being determined.

Compound F was also scanned to determine the nature of the structure as a function of emperature. This was accomplished using the Philips X-ray diffractometer, with a heating stage. The sample is mounted onto a thin aluminum plate and the then attached to the heating unit of the instrument. The diffractometer uses CuKα radiation. Dr. David Jenkins of the Geology Department at Binghamton University helped conduct the experiment. The sample was scanned at room temperature and then, starting at 200 °C, was scanned at 30 °C intervals up to 380 °C. The 2θ angles scanned were from 5 to 30 °2θ.

Compound A

Compound A was produced using a mixture consisting of V_2O_5(s) and LiOH(s) in ethylene glycol. Starting ratios of the solid V_2O_5 to LiOH were explored from 1:2 to 1:10. All of these ratios produced compound A. All of these ratios were investigated at a temperature of 200 °C in the traditional ovens with heat times of 2-8 days. There was an initial pH range of 5.1 to 10.3 depending on the LiOH content. The pH after synthesis was between 6.5 and 7.7. The method that produced the best powder sample of A is described below.

Twelve hours of stirring produced a moderately homogeneous mixture consisting of 300 mL ethylene glycol, 3.4 g of V_2O_5, and 0.567 g of LiOH. Having an initial pH of 10.3, four 75 mL portions were poured into four traditional oven vessels. The heat time for the vessels ranged from 2 to 8 days. The final pH readings ranged from 6.5-7.7. The sample that heated for 6 days produced the XRD pattern with the sharpest peaks.

A scan from 8-52 °2θ, was taken at a rate of 0.1 °2θ per second. A persistent second phase, evident in the XRD patterns by unindexed peaks of a different line width from the predominant material, seems to be the barrier prohibiting a successful, full characterization.. Presently alternate routes of synthesis are being examined to reduce the phase or better eliminate it.

Compound A was also scanned to determine the nature of the structure was as a function temperature. This was accomplished using the Philips X-ray diffractometer, with a heating stage. The diffractometer uses CuKα radiation. (Dr. David Jenkins and

Bill Blackburn of the Geology Department at Binghamton University helped conduct the experiment.)

Compound E

Material E was produced from a combination of 0.4 g of V_2O_5 in a solution containing 15 mL of distilled water and 35 mL of glacial acetic acid. That initial pH was 2.17, while the pH of the reaction solution was 2.16 after heating. Heating times of 2 and 4 days were explored, although no synthesis occurred at 2 days. An oven temperature of 165 °C was tested for two heating times. The first was heated for a single day and produced an orange and black material. The X-rayed material showed to contain strong vanadium pentoxide peaks. The sample that was heated for three days was pure black. However, that powder pattern also showed relatively intense peaks for the pentoxide as well.

The sample, originally made at 200 °C for 4 days, was X-rayed at a scan rate of 0.1 °2θ per min over the °2θ range of 8-52.

Sol-gel $Li_x V_2O_5 \bullet 2xH_2O$

Sol-gel $Li_xV_2O_5 \bullet 2xH_2O$ was synthesized only via microwave hydrothermal conditions. A 0.2g quantity of V_2O_5 was added to 12.5 mL of 1M LiOH. The pH was adjusted, by the addition of 3M acetic acid, to 3.5 and 2.9. The solutions were stirred for 12 hours and then reacted in the microwave vessel for 60 min. When the samples were removed from the drying oven they were bound to the filter paper in such a manner that removal was not possible.

Due to the difficulty of removing the sample from the filter paper, the XRD patterns were taken with the sample still on the filter paper. The X-ray sample was cut to fit the sample holder. Layers of double sided tape were used to raise the level of the sample to that of the holder's perimeter lip. (The height of the sample is an extremely important factor in resolving the sample's crystallographic structure.) That sample holders' contents were X-rayed from 2-60 °2θ, at a scan rate of 1 °2θ per min. The filter paper does not generate any scattering intensity, so its presence was insignificant.

There was no need to further the efforts with this sample because it showed to be of known composition. It was a lithiated version of sol-gel V_2O_5.

Chapter IV Results and Discussion

In this study of the hydrothermal formation of new vanadium oxides in the absence of the templating organic cation, five new compounds have been formed. Three of these have been completely characterized including the determination of their crystal structure. These three; vanadyl acetate, vanadyl glycolate, and trivanadium oxide hydrate will be discussed first followed by a brief discussion of the two remaining materials whose complete characterization will be performed by future researchers.

Compound C - Vanadyl Acetate - $VO(CH_3COO)_2$

Vanadyl acetate has a tan color, which had a greenish tint when acetic acid residue was present. An SEM image showed that it was comprised of long needles radiating from a single nucleation site as shown in the electron micrograph of figure 1c. The needles have dimensions of around 2 mm x 1 mm x 100 mm. The ends of the needles appear hexagonal. TheX-ray diffraction pattern indicated essentially a single phase with just a trace of V_2O_5. The vanadyl acetate was readily soluble in ethanol, glacial acetic acid and DMSO, while only slightly soluble in distilled water.

Thermal gravimetric analysis was used to determine the organic content. A weight loss of 51% was observed between 200 and 300°C, as indicated in figure 2c. This weight loss can be associated with the loss of the two acetate groups in $VO(CH_3COO)_2$. The X-ray diffraction pattern of the product, after the sample had been heated to 400 °C in a furnace for 2 hours, showed that the sample lost the organic and became fully oxidized to V_2O_5. This thermal data was consistent with the proposed composition. The conversion from the vanadyl acetate to vanadium pentoxide lead to a predicted weight loss of 50.8%, according to the following equation:

$$2\ [VO(CH_3COO)_2] + 17/2\ O_2 \rightarrow V_2O_5 + 8\ CO_2 + 6\ H_2O$$

The infrared spectrum in figure 3c showed the presence of a vanadyl group, with a band at 1029 cm^{-1},[33,34] a band at 895 cm^{-1} associated with a V-O bond, and a methyl group at 1462 cm^{-1}. The FTIR clearly indicated that the C-O bonds in the acetate group are equivalent. There was no peak present around 1800 cm^{-1} corresponding to a carbonyl

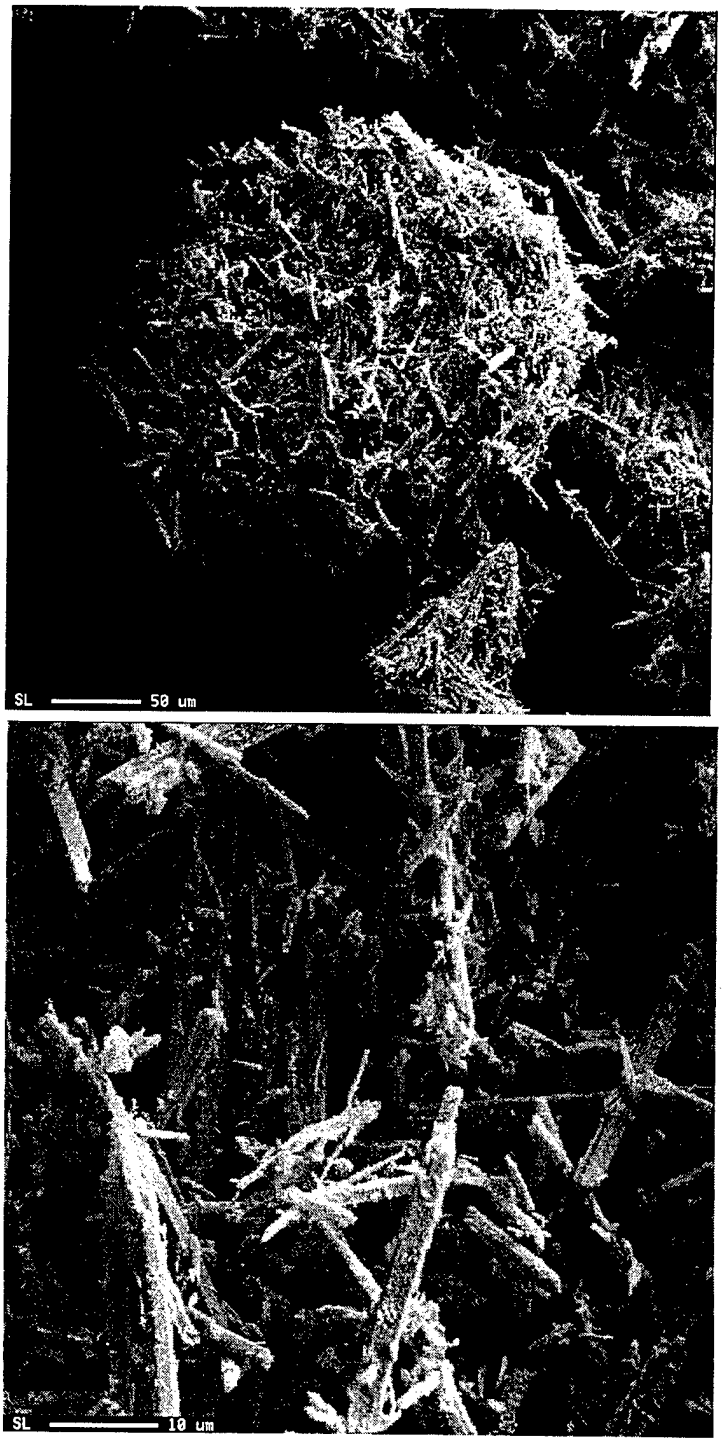

Figure 1c. The SEM images of the vanadyl acetate showing the individual fibers as well as their cluster configuration.

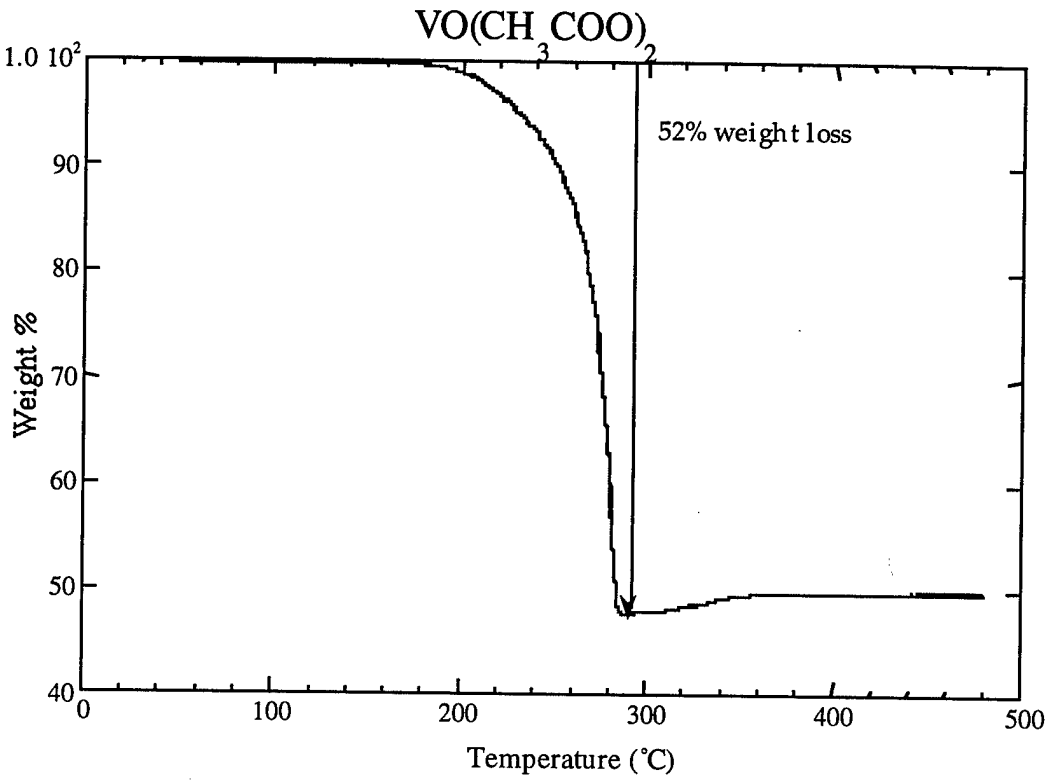

Figure 2c. The TGA plot of the vanadyl acetate under oxygen.

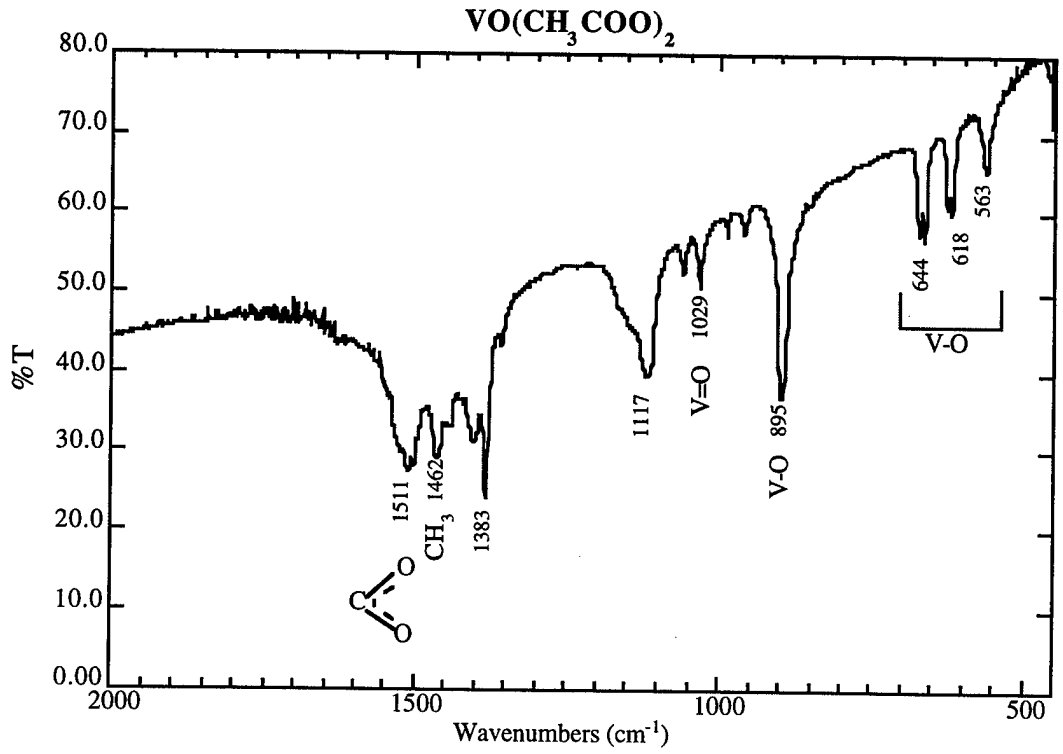

Figure 3c. The FTIR pattern of the vanadyl acetate.

stretch nor a peak indicative of a single C-O bond at around 1200 cm^{-1}. Instead there was a large peak about half way between them at 1511 cm^{-1}. It supported the idea of a resonating electron between two C-O bonds, thus giving a bond character of one and a half.

As noted earlier the color of the sample varied from a distinct tan to a greenish tan. The greener the material, the more acetic acid resided on the material. FTIR on the darker green samples showed very distinct carbonyl and C-O peaks. The spectrum of pure vanadyl acetate had neither a C=O or a C-O, but rather a single peak representing the resonating effect of the extra electron between the two C-O bonds in the acetate. The multitude of greenish tan shades were indicative of the difficulties encountered in attempts to rinse the sample of all acetic acid during filtration.

The X-ray powder diffraction pattern showed a d-spacing of 7.069 Å for the vanadyl acetate. The pattern was indexed with an orthorhombic symmetry and two possible space groups of CmC and $Cmc2_1$. The noncentrosymmetric $Cmc2_1$ was used to solve the structure. The lattice parameters are: a = 14.066(4) Å, b = 6.877(2) Å, and c = 6.926(3) Å. The profile fitting of the CSD program gave 140 integrated intensities. The powder X-ray diffraction pattern of the observed and the calculated data after the Rietveld refinement is shown in figure 4c. The first two reflections, below 18° 2θ, were excluded from the final refinement, because of their high intensity. The final refinement was done using the CSD program and is shown in table 1c. It gave $R_{(int)}$ = 0.070 and $R_{profile}$= 0.098. The calculated density of the acetate is 1.835 g/cc. The atomic position

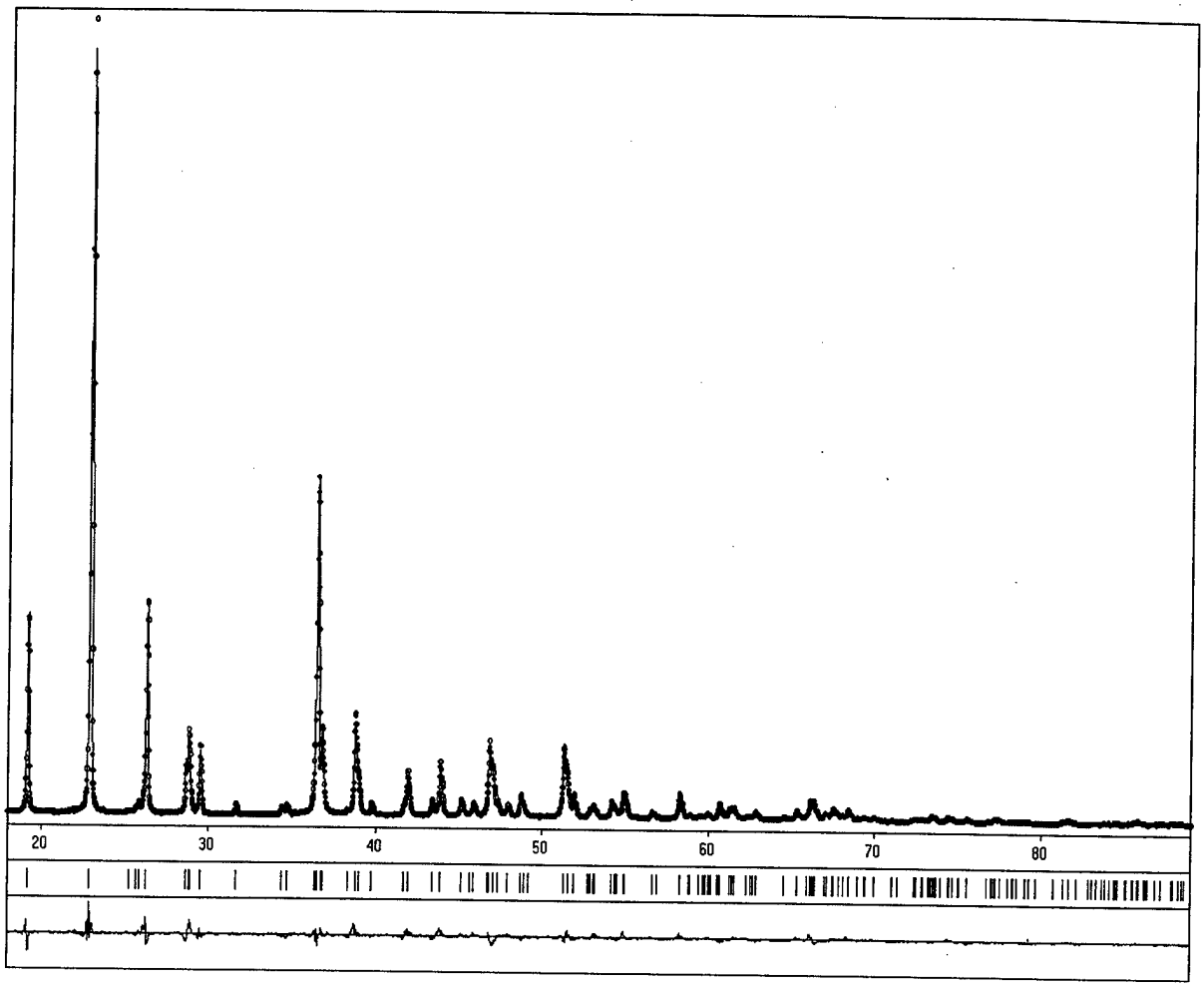

Figure4c. The calculated vs observed intensities for the vanadyl acetate.

Table 1c. The final parameters for the vanadyl acetate.

$VO(CH_3COO)_2$	
Space Group	$Cmc2_1$
a	14.0654(4) Å
b	6.8771(2) Å
c	6.9255(3) Å
β	90°
Cell Volume	669.9 $Å^3$
Z	4
F.w.	185 g/mol
Calculated Density	1.835g/cm^3
μ	121.7cm^{-1}
min, max 2θ	10,90
step 2θ, time	0.02, 30 sec
No. parameters	24
No. Reflections	155
R(B), R(exp)	0.070, 0.035
R(p), Rw(p)	0.098, 0.122

are described in table 2c. The V=O bond is 1.684(7) Å long consistent with other vanadyl bonds as found in layered vanadates, 1.37 Å to 1.69 Å, and 1.59 Å in the isolated cluster $[CH_3CN\subset(V_{12}O_{32}^{-4})]$.[37] The V-O bonds in the range of 1.931(4) to 2.131(7)Å are consistent with V-O bonds found in other layered vanadates.[28,33,34,35] A full listing of bond distances is shown in table 3c.

The structure of the vanadyl acetate can be described in two different ways. The first depicts the polyhedra as VO_5 square pyramids with a double bonded oxygen at the apex. That is consistent with the infra-red data. The square pyramids are joined together by the acetate groups to form one-dimensional chains as shown in figure 5c. The chains are comprised of offset square pyramids (SP). They are off-set in that one face aligns parallel to the base of the SP above it and so that one of its faces' aligns parallel to the SP below it.

The second way to describe the vanadyl acetate is to recognize the polyhedron as a distorted octahedral coordination of oxygen to the central vanadium atom. The octahedron would bond to each other along their axial vanadium oxide bonds in a corner sharing manner. The octahedron would angle so as to give a wavelike property to the chains. The bond distances given in table 3c support a single bond character with a bond length of 2.131Å between what, in the SP descriptions, would be the vanadium atom in one SP to the apex oxygen in the SP below.

The magnetic properties of the vanadyl acetate were investigated by magnetic susceptibility measurements and EPR spectroscopy. The evolution of molar magnetic susceptibility Xm as a function of temperature is represented in figure 6c. The

Table 2c. The atomic positions for the vanadyl acetate.

Vanadyl Acetate				
Atom	x/a	y/b	z/c	B(iso)
V	0	0.253(1)	0.5	2.20(3)
O1	0	0.1158(4)	0.7260(10)	1.49(9)
O2	0.1014(2)	0.1750(3)	0.040(7)	1.18(8)
O3	0.0928(2)	0.1814(4)	0.3652(7)	2.1(1)
C1	0.1322(2)	0.2276(5)	0.2094(12)	1.4(1)
C2	0.2969(2)	0.1002(4)	0.7003(9)	4.1(1)

Table 3c. The bond distances for the vanadyl acetate.

$VO(CH_3COO)_2$	
Bond	Length
V-O1	1.684(7)
V-O1'	2.131(7)
V-O2'	2.002(3)
V-O2"	2.002(3)
V-O3	1.931(4)

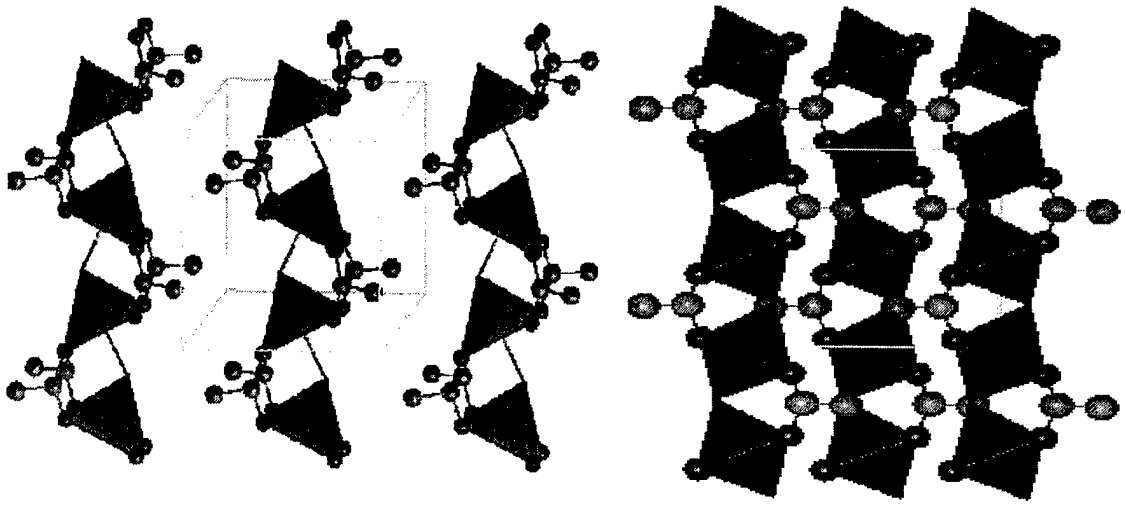

Figure 5c. Vanadyl acetate displayingboth SP and octahedral coordination of the vanadiums.

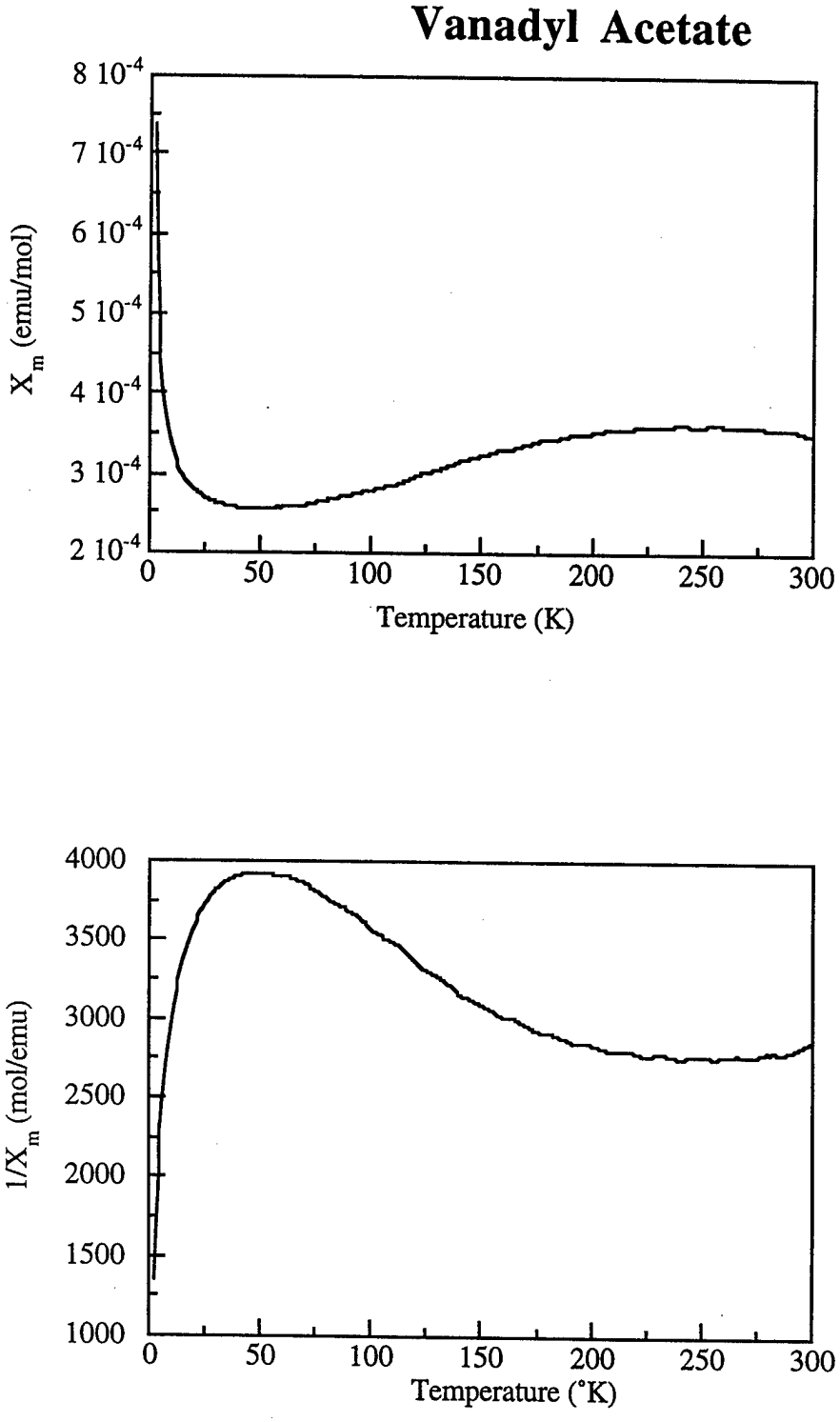

Figure 6c. Magnetic susceptibility results for the vanadyl acetate.

susceptibility exists as a Curie-Weiss like behavior only in the short temperature range between 2 and 15 K. That indicated the existence of isolated spins (or weakly interacting.) For a temperature range higher than 50 K, a wide bell-like curve was observed, which exhibits a maximum around 250 K. The latter signal could be attributed to an antiferromagnetic behavior, probably along the chains.

The EPR signal, recorded at room temperature, is shown in figure 7c. The signal has an intense isotrope with a relatively narrow linewidth of 68.4 Gauss and a g-factor equal to 1.966 which was really close to that found for the parent V_2O_5. The signal confirmed the existence of unpaired electrons, which was consistent with the near V^{+4} oxidation state of the sample.

The electrochemical activity of the material was explored using the MacPile collecting program described in the experimental section. The cathode was not easily reduced. Thus, the electrochemical reaction with lithium resulted in less that 0.1 lithium ions per vanadium being consumed above an emf of 2 volts.

In summary, in an attempt to synthesize multidimensional compounds in the absence of templating, or structure directing organic cations, a chain like vanadyl acetate was produced. The chains are one dimensional and exhibit little interaction between the chains. Acetate groups provide the bridging groups through the equatorial oxygen sites of one polyhedron to the ones above and below. The bond lengths support a vanadyl bond, but also supports a single bond character from the vanadium to the oxygen below it. The

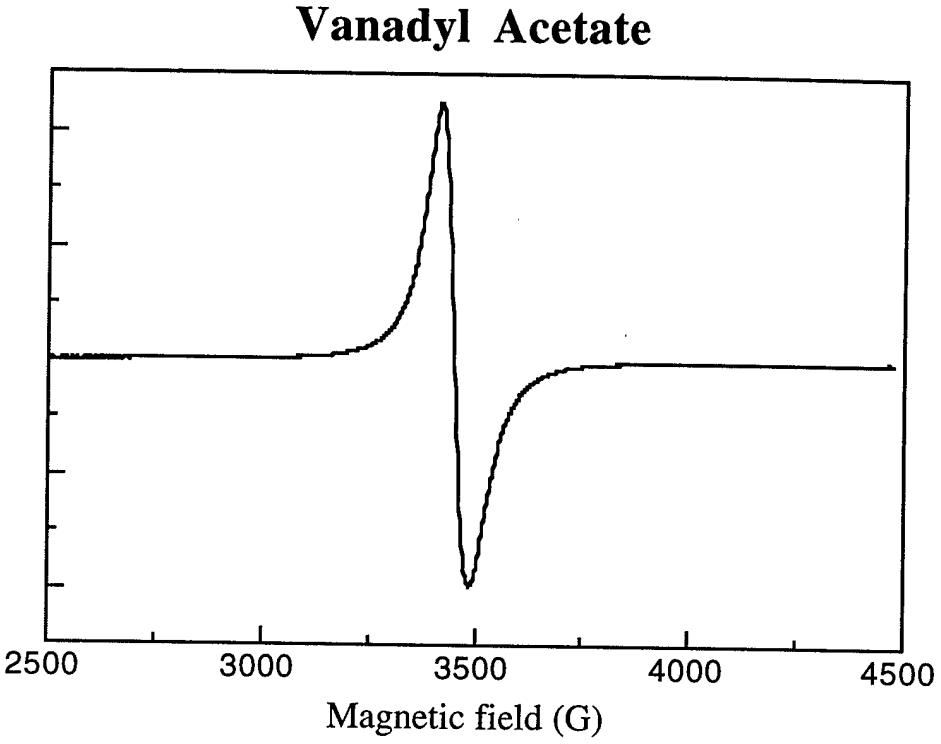

Figure 7c. EPR results for the vanadyl acetate.

FTIR data showed support for the vanadyl, but also had many peaks attributed to several single bonds.

A vanadyl acetate had previously been reported in Ghana J. Chem, but it was not an obtainable publication.[38]

Compound B - Vanadyl Glycolate - $VO(OCH_2CH_2O)$

The vanadyl glycolate has a purple color, which upon prolonged exposure to air turned black. This color indicates that the vanadium was reduced from V^{+5} to V^{+4} during the synthesis, with a slight oxidation occurring exposure to air. X-ray, TGA and FTIR analysis showed no obvious difference between the purple and black colored samples. The electron microscope images do not offer the best resolution, but clearly depict the fiber-like strands as shown in figure 1b. Those strands correspond to growth in the 001 direction, down the long axis of the chains, as expected from the crystal structure. The glycolate was readily soluble in acetic acid and ethanol, while extremely soluble in DMSO It showed to be nearly insoluble in distilled water.

The powder X-ray diffraction pattern of the vanadyl glycolate showed a d-spacing of 6.635 Å. The pattern was indexed with a monoclinic system, and assigned to be C2/c. The lattice parameters for the glycolate are: a= 9.2707(4) Å, b=9.7345(9) Å, and c=9.9132(8) Å where β=106.03°. (The a and c parameters were switched so as to keep the convention of having the unique angle b, describing the angle between the a and c axis of the unit cell.) The X-ray diffraction pattern, upon indexing, gave 261 integrated intensities. The calculated vs. observed intensity data after the final Rietveld refinement, shown in figure 2b, was obtained by using the CSD program and is described in table 1b. The calculated density of the new compound is 1.962 g/cm^3. The atomic positions are described in table 2b. The bond distances of the vanadyl group are

Figure 1b. SEM image of the vanadyl glycolate.

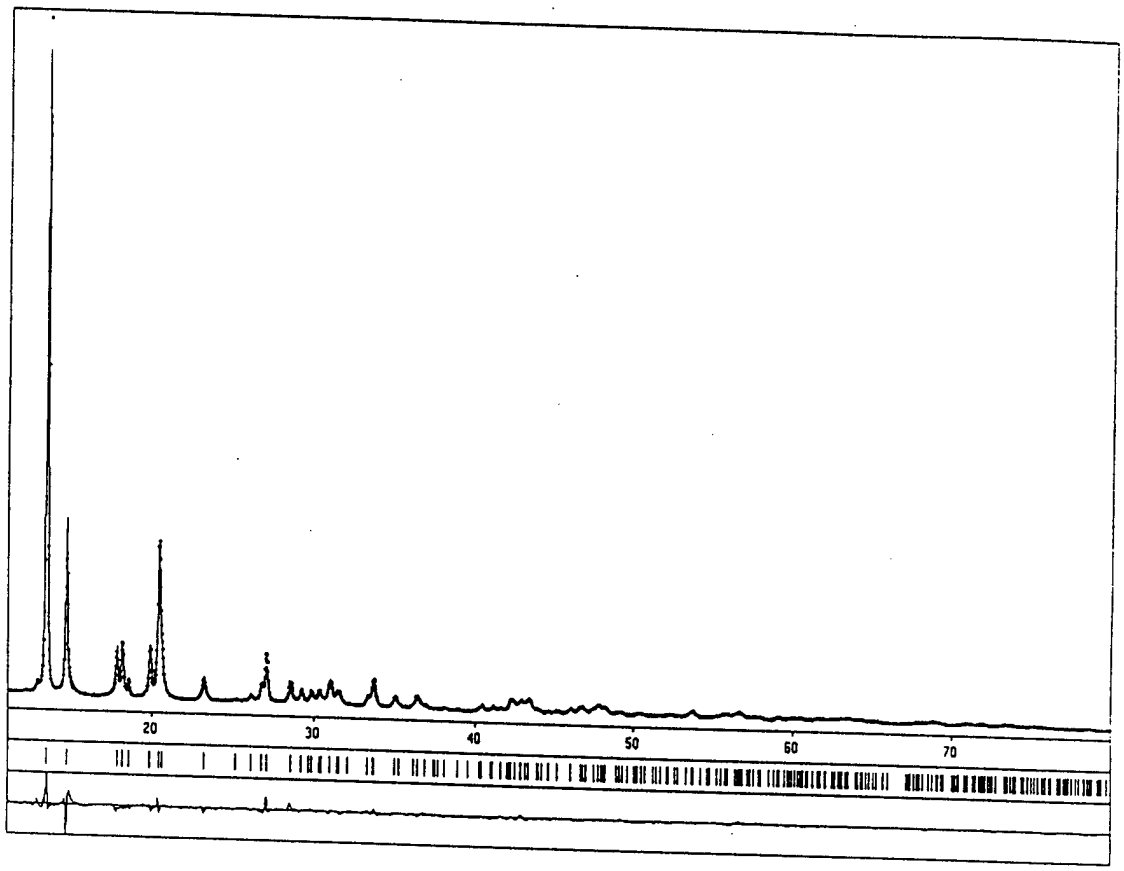

Figure 2b. The calculated vs observed intensities for the vanadyl glycolate.

Table 1b. The final parameters for the vanadyl acetate.

$VO(OCH_2CH_2O)$	
Space Group	C2/c
a	9.2707(8) Å
b	9.7345(9) Å
c	9.9132(8) Å
β	106.029°
Cell Volume	859.8 $Å^3$
Z	8
F.w.	127 g/mol
Calculated Density	1.962/cm^3
μ	183.3cm^{-1}
min, max 2θ	8,80
step 2θ, time	0.03, 35 sec
No. parameters	42
No. Reflections	261
R(B), R(exp)	0.061, 0.033
R(p), Rw(p)	0.105, 0.108

Table 2b. The atomic positions for the vanadyl acetate.

Vanadyl Glycolate				
Atom	x/a	y/b	z/c	B(iso)
V	-0.0165(5)	0.129(4)	0.0917(5)	.086(7)
C1	0.271(3)	0.030(2)	0.270(3)	4.4(8)
C2	0.279(3)	0.016(2)	0.132(2)	3.4(8)
O1	-0.0115(9)	0.2673(12)	0.0192(11)	1.3(3)
O2	0.143(2)	0.1002(11)	0.2785(13)	1.9(4)
O3	0.1286(14)	0.232(2)	0.032(2)	2.3(4)

Table 3b. The bond distances for the vanadyl glycolate.

$VO(OCH_2CH_2O)$	
Bond	Length
V-O1	1.576(12)
V-O2	2.037(14)
V-O2'	1.976(15)
V-O3	1.888(15)
V-O3'	1.981(15)
C1-C2	1.40(4)
C1-O2	1.39(3)
C1-O3	1.47(3)

1.576 Å and the range of vanadium oxygen bonds is between 1.888 and 2.037 Å. A summation of the bond length for all atoms is described in table 3b. The sample had a strong preferred orientation in the 00l direction. The preferred orientation was determined from the characterization of the material. The chains consist of an array of vanadium atoms coordinated to five oxygens forming a square pyramid (SP). The SPs are composed of a vanadyl group (V=O) and 2 chelating (-O-CH_2-CH_2-O-) ligands. The vanadium double bonded to oxygen occupies the apex of the SP. The presence of that vanadyl group was supported by the FTIR spectrum of the sample. The FTIR spectrum, shown in figure 3b, depicts an intense absorption peak at 1005 cm^{-1}. This feature is characteristic of the V=O stretch in many other vanadium oxides. It is present at 1022 cm^{-1}, 1009 cm^{-1} and 996 cm^{-1} respectively in V_2O_5, $Li_xV_{2-\delta}O_{4-\delta} \cdot H_2O$, and $TMA_x V_8O_{20}$.[33, 35]

The chelating glycolate ligands, which are the second component of the polyhedron, run continuously throughout the chains and comprise the base of the pyramids. The 4 oxygens making up the plane of the base are flat, but the two (CH_2) groups do not lie directly below their respective oxygens. The arc of the carbon chain angles away from the vanadium chain direction. The presence of (V-O) bonds were also supported by the FTIR. They are present as peaks at the low wavenumbers end of the spectrum as seen in the vanadyl acetate's spectrum. [33,34,35] The presence of the CH_2 bonds are also visible in the FTIR spectrum at 2939 cm^{-1} .[39]

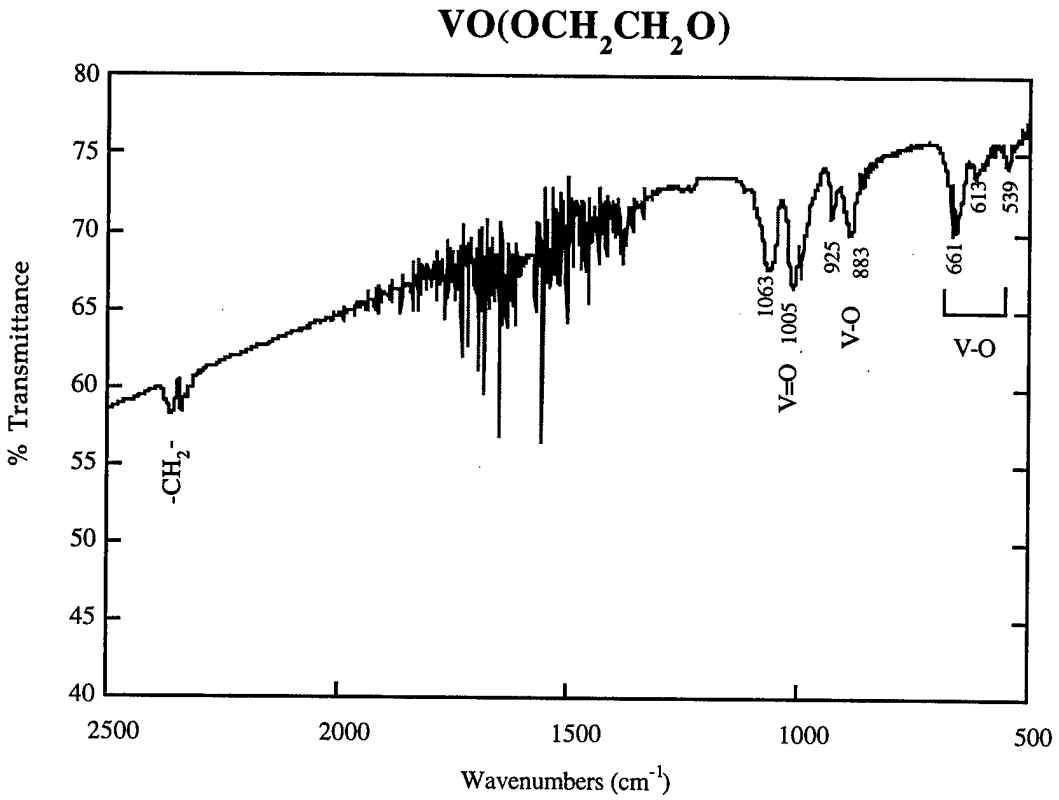

Figure 3b. FTIR spectrum of the vanadyl glycolate.

The square pyramids share two common oxygens, which are referred to as edge sharing. The structure, in figure 4b, depicts the pairing of the SPs in the chains. There are two apices pointing "up" and two pointing "down" in a continuous manner. The paired vanadyl groups point slightly away from each other in both the up and down directions. That produces a wavelike appearance in the chains.

The use of the TGA data offered some information in the prediction of an approximate composition of the B material. The sample was scanned from 50-450 °C at 1 °C per minute. The sample showed a weight loss of 33.4 % from 50 °C to 190 °C, as seen in figure 5b. The weight loss could be explained by the presence of the organic component of the sample and to any bound or adsorbed water. With the boiling point of ethylene glycol being 185 °C and there being a large weight loss at about that temperature, it made sense that there was some form of ethylene glycol in the sample.

The TGA was helpful in deciphering the oxidation state of the transition metal. The plateau in the scan between 190 and 300°C was over a substantial temperature range and allowed the determination of the intermediate phase present. A 60-80 mg portion of the vanadyl glycolate was heated in a tube furnace at 230 °C for 2 hours. The black sample was X-rayed and characterized as VO_2 by using the JCPDS files. Another portion, of roughly the same size, was heated to 400°C for 2 hours, and the bright orange sample was found to be V_2O_5. It too was referenced using the JCPDS files.

Vanadyl Glycolate

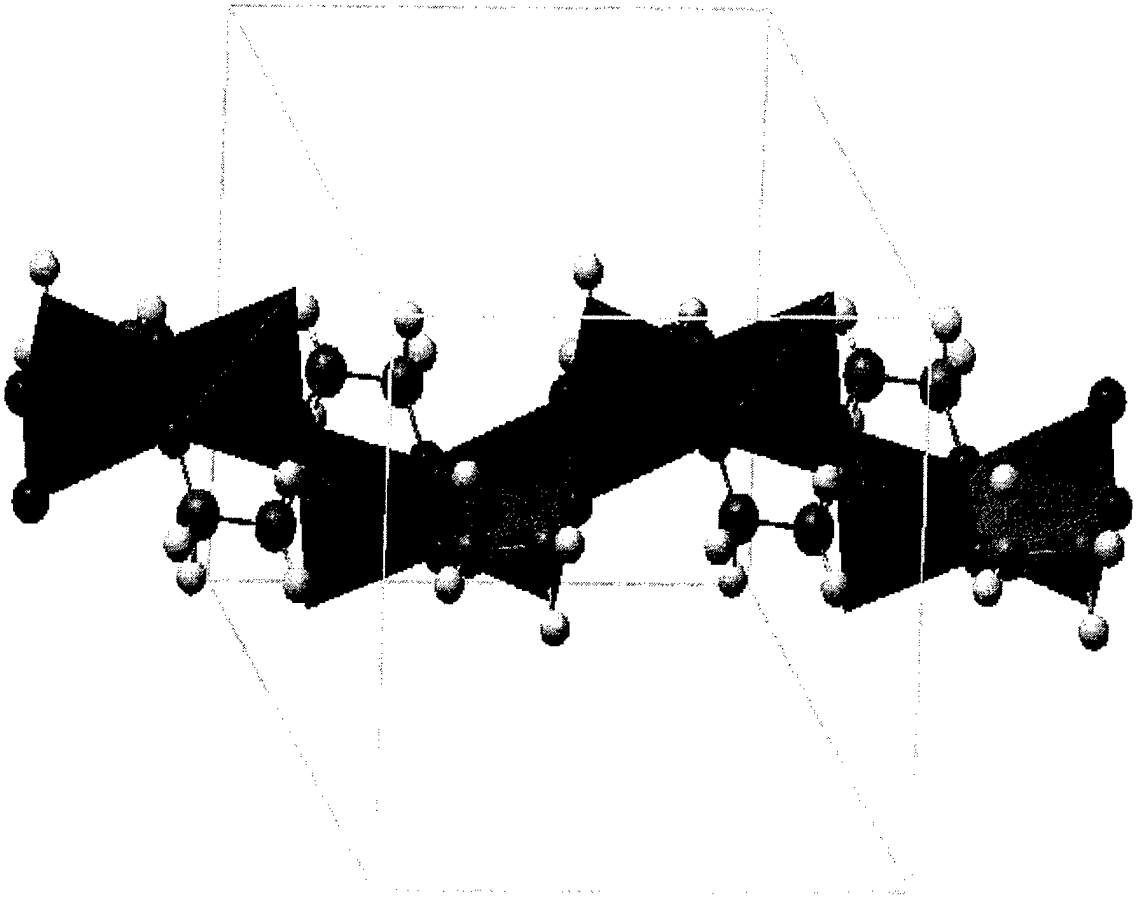

Figure 4b. The 1-dimensional chain structure of $VO(OCH_2CH_2O)$.

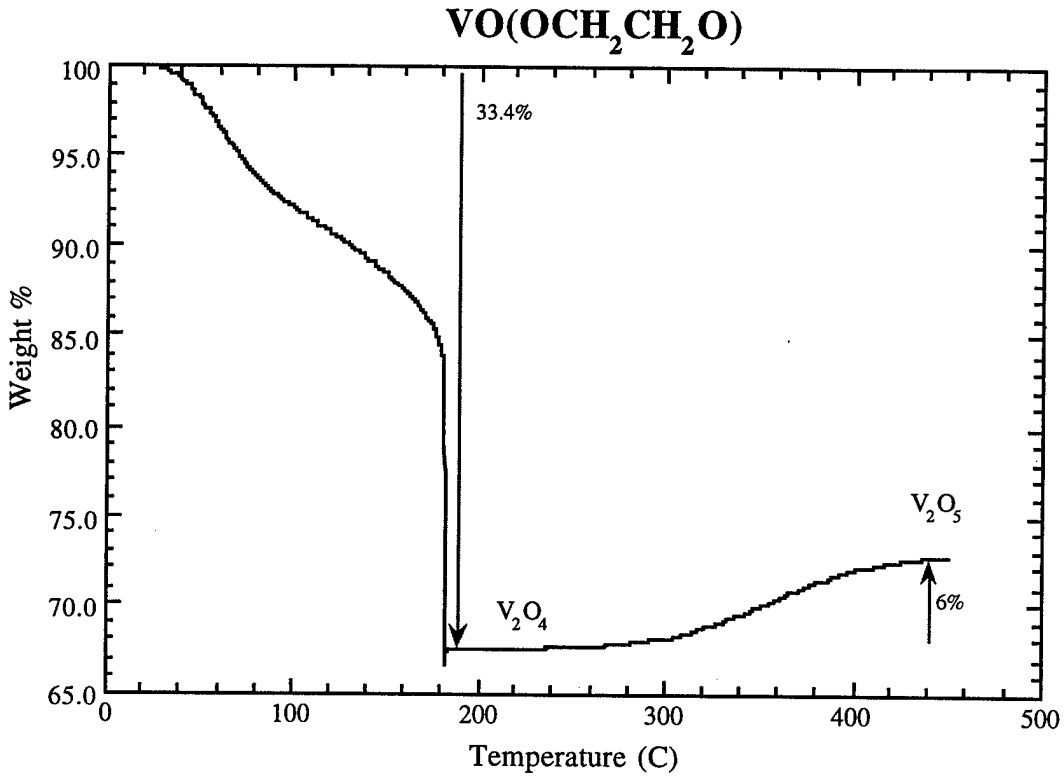

Figure 5b. TGA plot of the vanadyl glycolate.

The two key features in the TGA plot can be associated with loss of the organic, a stable intermediate region followed by oxidation of the V_2O_4 to V_2O_5 as indicated below:

1. a loss of organic and a conversion to V_2O_4

$$2\ [VO(OCH_2CH_2O)] + 5\ O_2 \rightarrow V_2O_4 + 4\ CO_2 + 4\ H_2O$$

The calculated weight loss is 34.6% which compares well with the 33.4% observed loss.

2. the conversion to V_2O_5

$$V_2O_4 + 1/2\ O_2 \rightarrow V_2O_5$$

The conversion to the pentoxide would be the addition of 1/2 mole of O_2 to the V_2O_4. which corresponds to an 8.8% weight increase.

The magnetic properties of the glycolate were investigated by magnetic susceptibility measurements and EPR spectroscopy. The plot of the molar susceptibility as a function of the temperature is shown in figure 6b. It exhibits a Curie-Weiss like behavior in the temperature range of 2-300 K, but the plot of the inverse susceptibility, as a function of temperature, only shows linear behavior between 175 and 300 K. The range below 175 K shows a negative deviation in the line. The fit of the line between 175 and 300 K gives the following values for the Curie and Weiss constants:

C=0.145 emuK/mol $\qquad\qquad$ θ=-76K

The EPR signal of the glycolate, at a room temperature scan, showed a Lorentzian isotropic line characterized by a linewidth of 160 Gauss and a g-factor of 1.97 (which is equal to that for V_2O_5 powder.) This was consistent with the Curie-Weiss like behavior observed in the susceptibility measurements. The plot is shown in figure 7b.

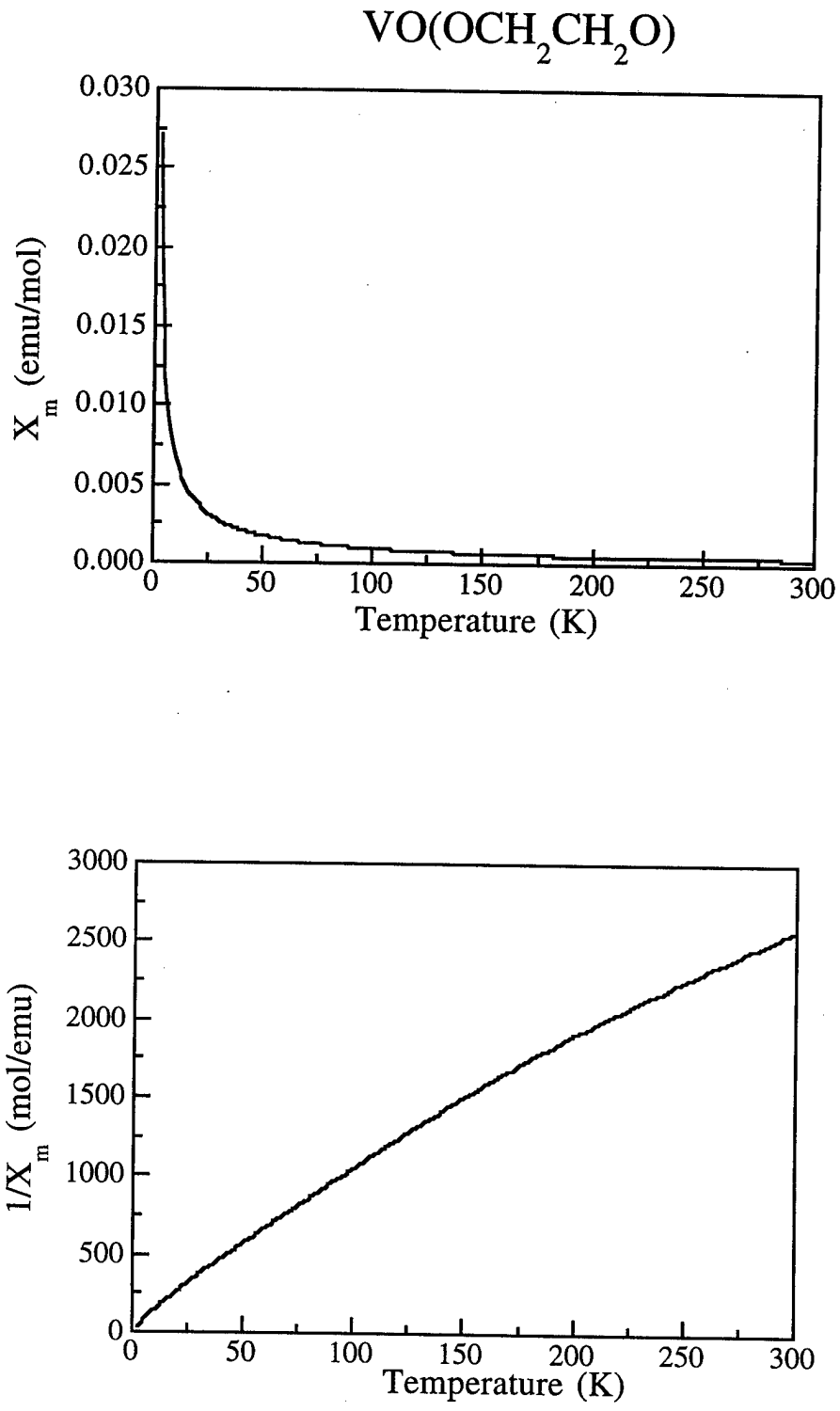

Figure 6b. Magnetic susceptibility results for the vanadyl glycolate.

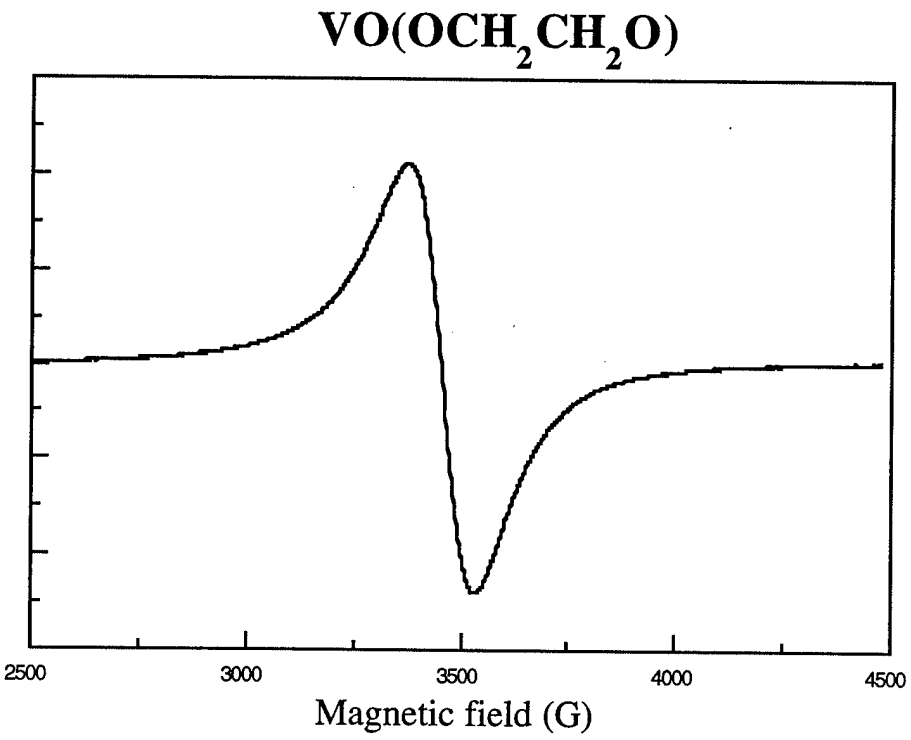

Figure 7b. The EPR data for the vanadyl glycolate.

In summary, a new vanadyl glycolate has been synthesized and characterized. The vanadyl glycolate, with the chelating glycolate in the structure, showed a bridging nature. Ethylene glycol was used with partial anticipation that its two terminal oxygens would offer themselves as sites for an interlayer bridge between the two vanadium oxide sheets. The preceding structural determination of the vanadyl acetate material led to the observance of the bidentate ligand. The vanadyl acetate shows a structure with vanadium in octahedral coordination. The comparison between the two arrangements of the starting solvents: acetic acid and the ethylene glycol show a difference of potential binding sites (see figure 8b.) The acetic acid offers two oxygen atoms on the same end of the carbon chain where the ethylene glycol offers two oxygens at opposite ends of the chain. The chain of 2 carbon atoms, in ethylene glycol would seem to have more flexibility than a chain of 1 carbon. The flexibility being in the additional bond (2 vs. 3). In recognition that and the extended length, it was thought that perhaps one glycolate could bend so that the two terminal oxygens offered an appropriate orientation to allow for bonding to the transition metals.

Acetate

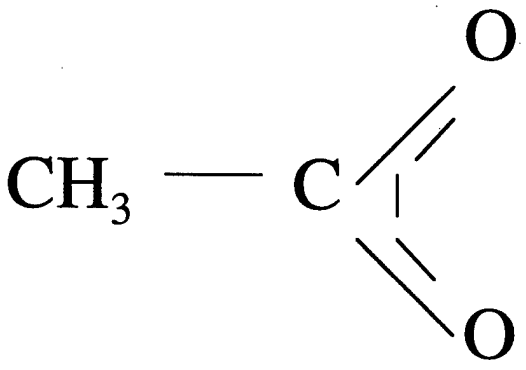

Glycolate

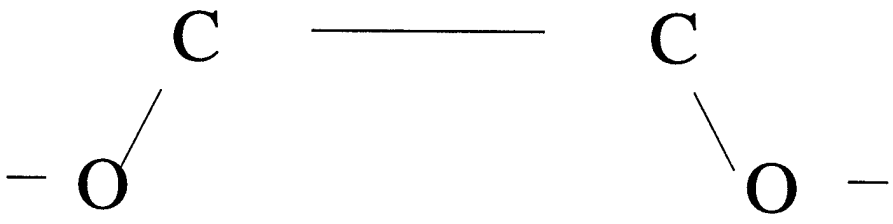

Figure 8b. The two different ligands that comprise the chain materials.

Compound F - Trivanadium Oxide Hydrate - $V_3O_7(OH_2)$

This compound was consistently black upon synthesis. Since there was not a bright orange color, the vanadium had become reduced during the synthesis from the fully oxidized V^{+5} in V_2O_5. The black powder looked very granular upon filtration. It was a fine powder to start with, so grinding with mortar and pestle had little affect. The material was very soluble in acetic acid, ethanol, DMSO and distilled water. The SEM image of the layered $V_3O_7(OH_2)$ compound, in figure 1f, did not indicate a strongly layered compound. The long fiber-like material appeared to have an average length of 50 mm.

The thermal gravimetric analysis in oxygen showed there to be a weight loss of 3.5% up to 300 °C, followed by a weight gain as shown in figure 2f. A weight loss of 6.3% would be expected if there was a loss of the water component of the compound, and an over all weight loss of 6.7% for the conversion of the compound to pure V_2O_5. Thus, partial oxidation of the vanadium must have occurred concurrently with dehydration up to 300 °C, possibly by abstraction of some of the hydrogens by atmospheric oxygen. The sharp weight gain between 300 °C and 360 °C was the complete oxidation to V_2O_5, which showed its characteristic bright orange color. These changes could be associated with the following reactions:

$$V_3O_7(OH_2) \Rightarrow H_2V_3O_8 \cong V_3O_{8-\delta} \cong V_2O_5$$

The lack of any intermediate products during the thermal analysis, which indicated a transition from the $V_3O_7(OH_2)$ to pure V_2O_5, was confirmed by taking X-ray scans of

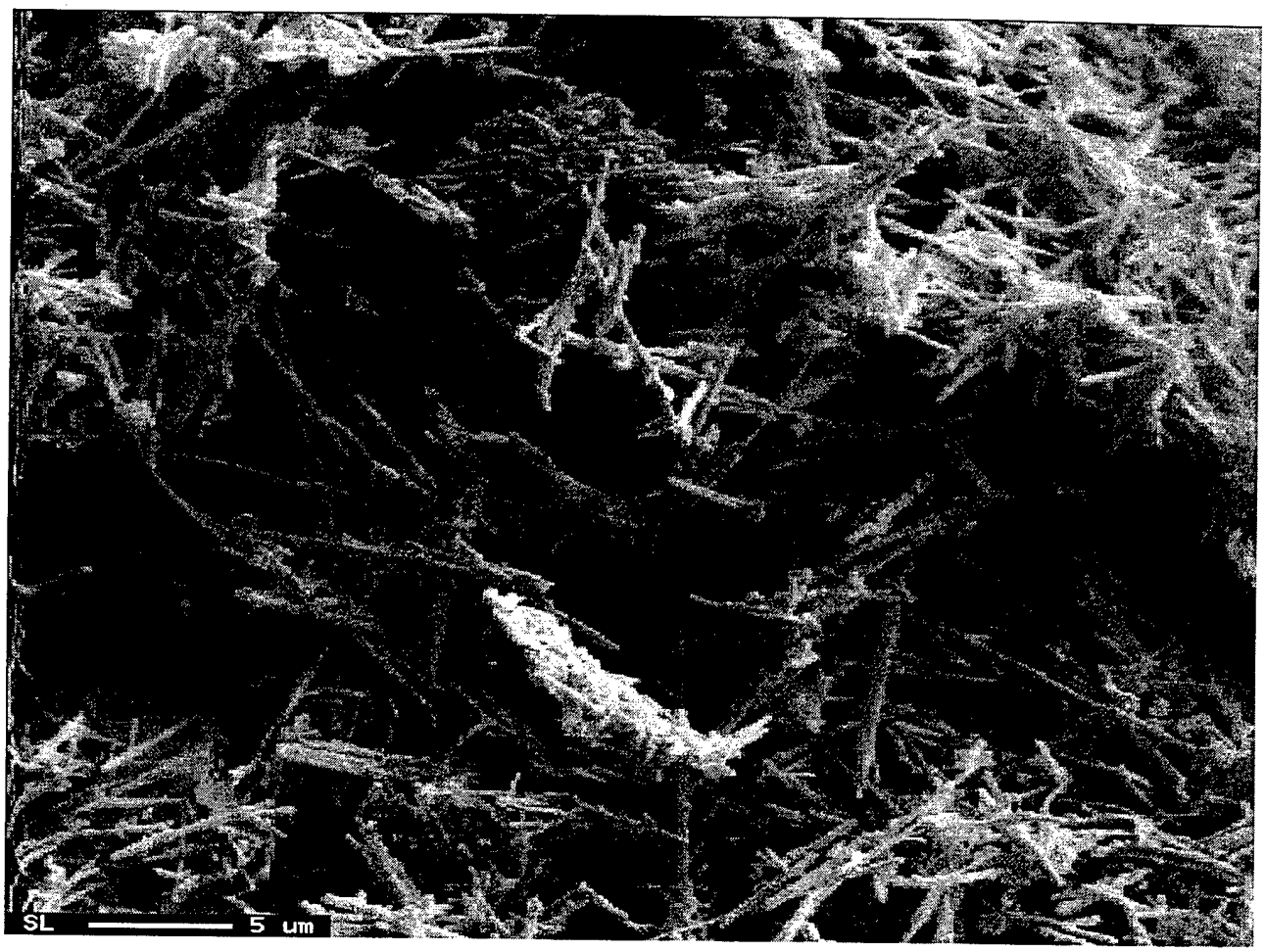

Figure 1f. SEM image of $V_3O_7(OH_2)$

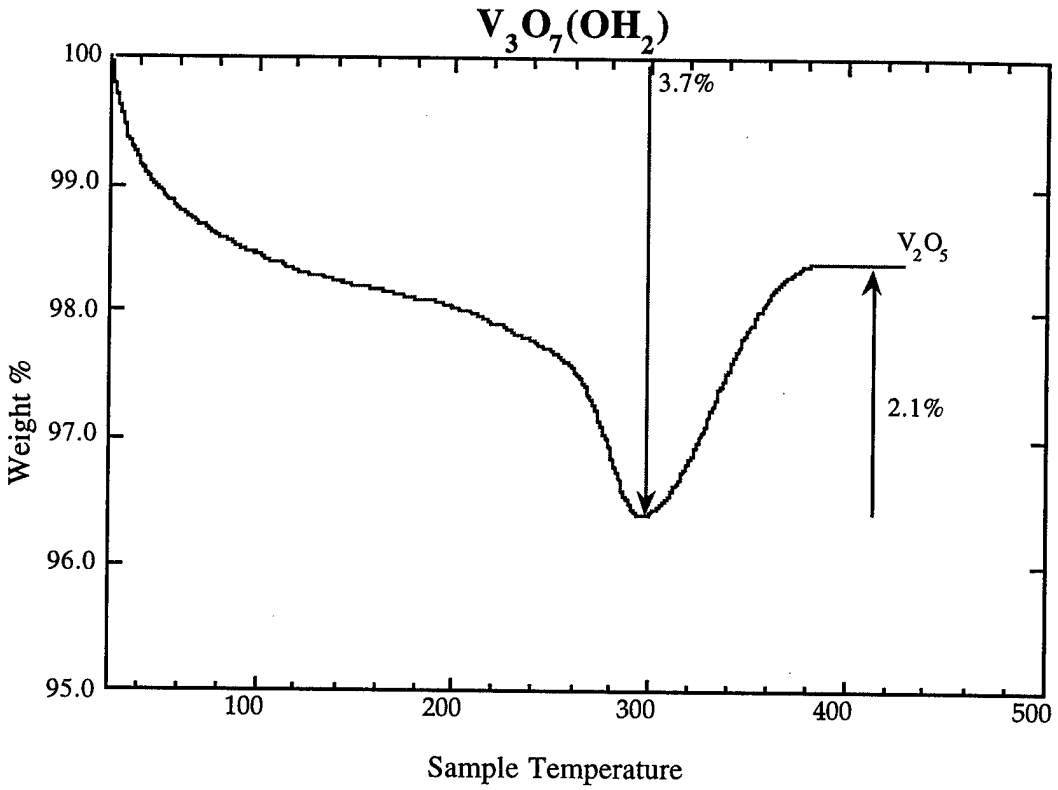

Figure 2f. Thermalgravimetric data for the trivanadium oxide hydrate.

the sample as a function of temperature from 25 °C to 380 °C. That transition occurred around 300 °C and was seen in the XRD pattern as a loss of the peak at 8.53 Å and an increase of peak at 5.77 Å, corresponding to a loss of the $V_3O_7(OH_2)$ and an increase of V_2O_5.

The powder X-ray diffraction pattern showed a d-spacing of 8.519 Å. The sharp peaks indicated that a highly crystalline materials was present. The pattern was indexed with an orthorhombic system, and with the space group Pnam using the CSD program. The lattice parameters for the hydrated vanadium oxide are: a= 16.9298 Å, b=9.3589 Å, and c=3.6443 Å. The powder X-ray diffraction pattern is shown in figure 3f. The final refinement was accomplished also using the CSD program. The calculated density of the new compound was 3.253 g/cm^3. The V=O had a bond distance of 1.590 Å and the single V-O bonds ranging between 1.816-2.473 Å. These were consistent with other vanadium oxides. [33,34,37,40]

The structure of the sample is a layered array of clusters of vanadium atoms linked together by square pyramids that alternate up and down. There is an interlayer attraction that occurs due to weak hydrogen bonding. The clusters are composed of 4 vanadium molecules octahedrally coordinated to oxygen. These 4 octahedron are linked to each other by corner edge and corner sharing. Each octahedron shares an equatorial edge to one adjacent octahedron, and corner shares to the one in the plane with it. It does not bond to the other octahedron. In the clusters there are two different vanadium sites. The octahedron that do not touch each other are the same. That is in both directions across

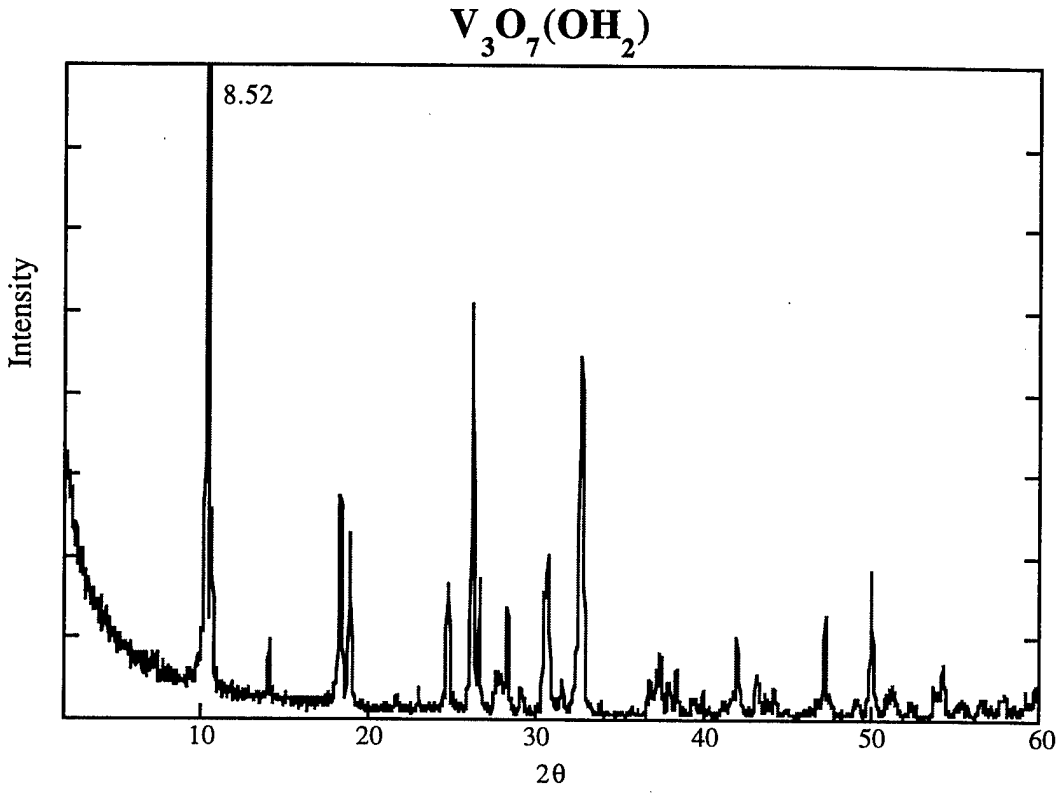

Figure 3f. The powder X-ray diffraction pattern of the trivanadium oxide hydrate.

the cluster. The reason that they are different is that the hydrogen bonding occurs off of two of the four octahedron. (Hydrogen bonding effects all 4 of the vanadium polyhedra, but two from the cluster posses the oxygen end of the bound water and two receive the hydrogen end of the water.) Two "nontouching," similar octahedron, have the oxygen that are from the bound water. The extending hydrogen participates in the hydrogen bonding to octahedron from another layer, and thus another cluster that is close and has an oxygen extending towards the water. These are clearly depicted in an image of the structure in figure 4f. The alternating SPs are aligned so that their bonding occurs from the corner of one SP to the edge sharing portion of one cluster and from the other corner of the second SP to another cluster in the same layer. The SPs edge share to each other. The cluster of 4 has two different types of vanadiums, as mentioned, and then there is a third type in the SP coordination. Therefore there are three distinct vanadium sites in $V_3O_7(OH_2)$. The octahedrally coordinated vanadiums are in an oxidation state of V^{+5} and those with the SP are in a V^{+4} state. Since there are twice as many vanadiums in the V^{+5} state, the net oxidation state of the transition metal is $V^{+4.67}$.

The FTIR spectrum, in figure 5f showed support for the presence of vanadyl group (V=O) with the peak at 1024 cm^{-1}. That was a bit higher than expected, but was still close to that in vanadium pentoxide.[41] The FTIR data for this sample was less supportive than for the two vanadyl species.

The magnetic properties of $V_3O_7(OH_2)$ were studied by EPR spectroscopy and susceptibility measurements. The evolution of the molar magnetic susceptibility, as a

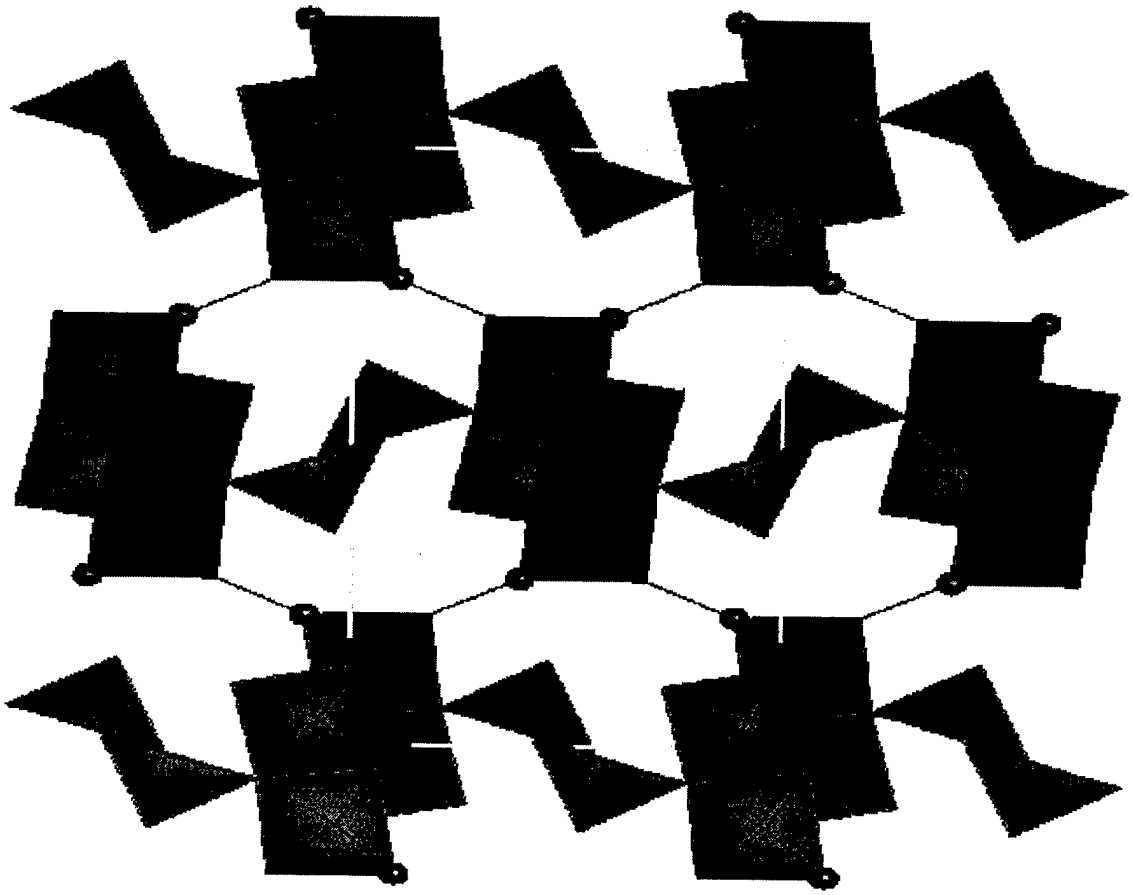

Figure 4f. The structure of the trivanadium oxide hydrate.

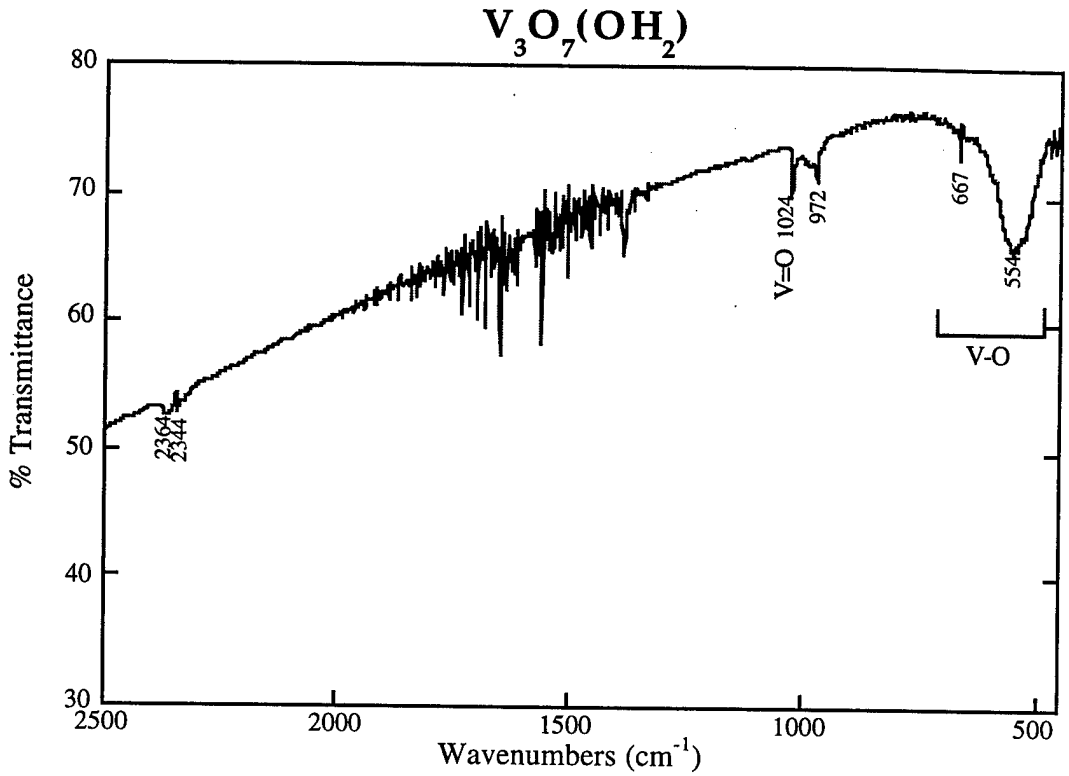

Figure 5f. The FTIR spectrum of $V_3O_7(OH_2)$.

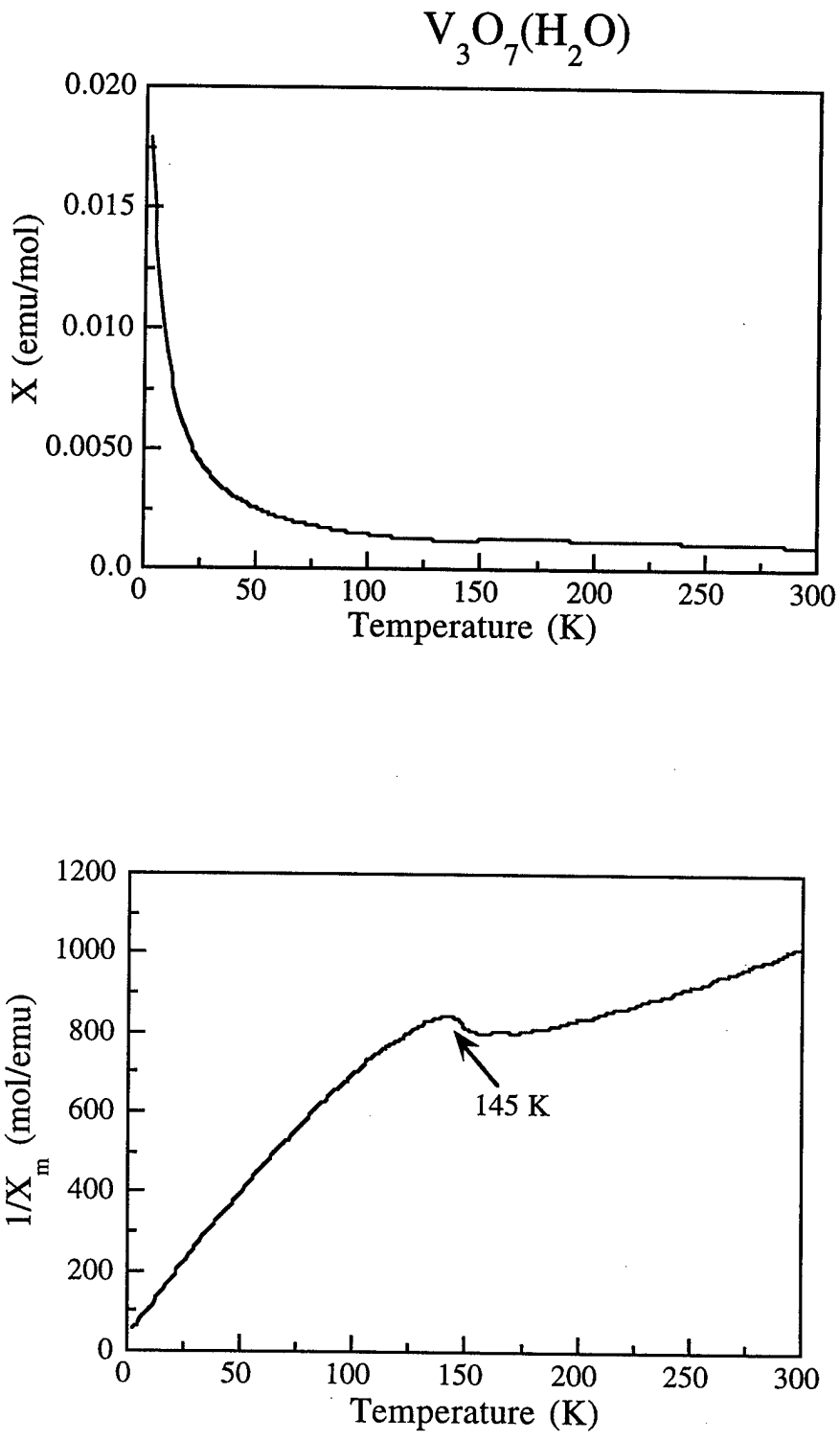

Figure 6f. The susceptibility data for the $V_3O_7(OH_2)$.

function of T is shown in figure 6f. The curve seemed to follow a Curie Weiss like behavior in the entire temperature scan. However, the fit of the curve showed the existence of a positive deviation for a temperature higher than 140 K. The plot of the inverse susceptibility magnifies these features showing the existence of two dissimilar behaviors on either side of 140 K. This could result from the existence of a phase transition. DSC, at low temperature, would be necessary for confirmation.

The EPR spectrum is represented in figure 7f. It consisted of a broad signal with a linewidth of 315 Gauss. The signal showed a relatively high signal to noise ratio. The g-factor was found to be 1.95, a little lower than that of the vanadium pentoxide powder.

The electrochemical activity of the material was explored using the MacPile collecting program described in the experimental section. The electrochemical results will be reexamined to explore an error in the first trial.

In summary a vanadium oxide hydrate, $V_3O_7(OH_2)$, has been formed from V_2O_5, and its mode of thermal decomposition and crystal structure determined. Fransisco Theobald in France[30] first reported the formation of $V_3O_7(OH_2)$. It was synthesized by hydrothermal means, but not in a Teflon liner. Their procedure differed mainly in the vessel type and the fact that they had to heat the vessel up to 450 °C. This compound was later synthesized and the structure determined by Oka, Yao, and Yamamoto in 1990.[40] Their preparation started with vanadium in a reduced state: heating of an aqueous solution of $VOSO_4$ at 200°C. Our procedure was simpler and at a lower temperature. They characterized it with the same structural parameters as this work, and our electron

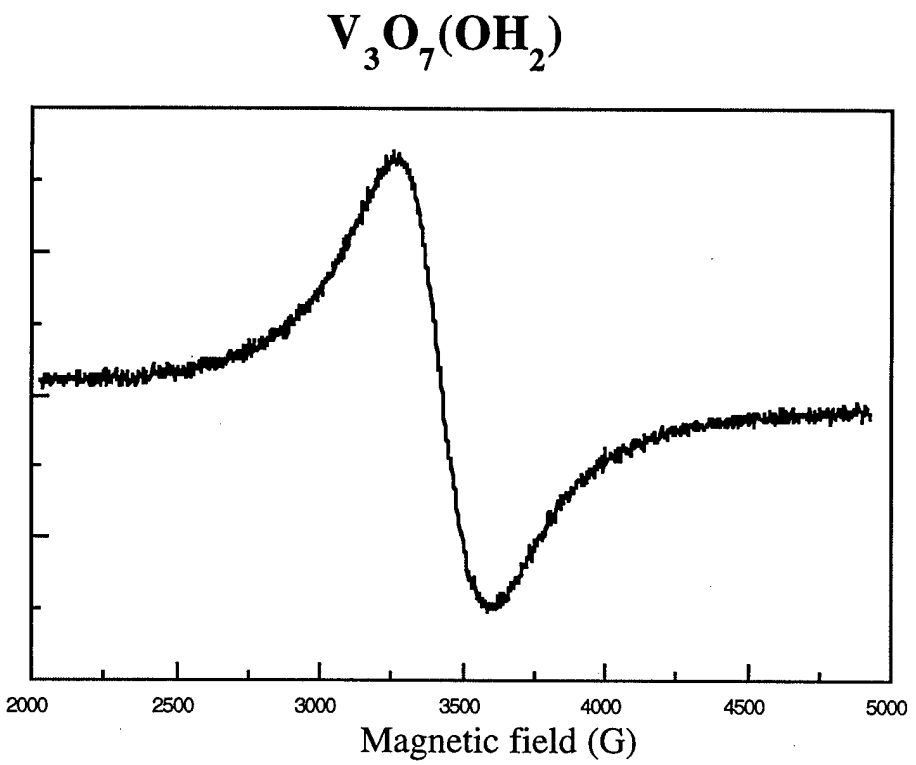

Figure 7f. The EPR results of the trivanadium oxide hydrate.

micrographs were similar to theirs. They describe the bonding between the cluster chains as trigonal bipyramidal instead of SPs. Currently work is being conducted to investigate the feasibility of making it via microwave hydrothermal means.

Compound A

Material A's dark colors of blue and black, suggest that the oxidation state of the vanadium atoms were not V^{+5}, but rather between V^{+4} and V^{+5}. The color of vanadium species with V^{+3} are often dark bluish in color. The SEM images of the material, such as in figure 1a, show a layered composition. The structures that appear to be flaky and packed in stacks.

The thermal analysis of the sample, represented in figure2a, showed there to be a modest weight loss of 9.3% that could be described as a loss of organic. The final product of the sample, after being heated in the flow of oxygen gas, was vanadium pentoxide. The curve resembled that of the glycolate, but did not have as much weight loss. An expected percent weight increase, indicative of that for the formation of pentoxide formation, was not observed. A comparison of this TGA data with the glycolate was crucial because the starting materials of the two were very similar.

The XRD pattern of the material showed a d-spacing of 8.037 Å in figure 3a. The material showed a high crystallinity. There may be a second compond in the powder causing difficulty in the crystallographic interpretation of the data. Work continues in trying to purifying this compound.

The FTIR spectrum, in figure 4a, showed the presence of vanadium oxide bonds at low wave numbers. The peak at 991cm^{-1} could represent a V=O bond. That is slightly lower than the 1005 cm^{-1} found in the glucolate. The peaks at 1063 and 883 cm^{-1} were common to other spectra as well.

The EPR data showed there to be the presence of a broad signal that represents paramagnetic vanadium with its 207.2 Gauss linewidth. An 0.2 gram portion of the sample was examined at a frequency of 9.526 (GHz) with the maximum at a field of 3463 G. It is shown in shown in figure 5a.

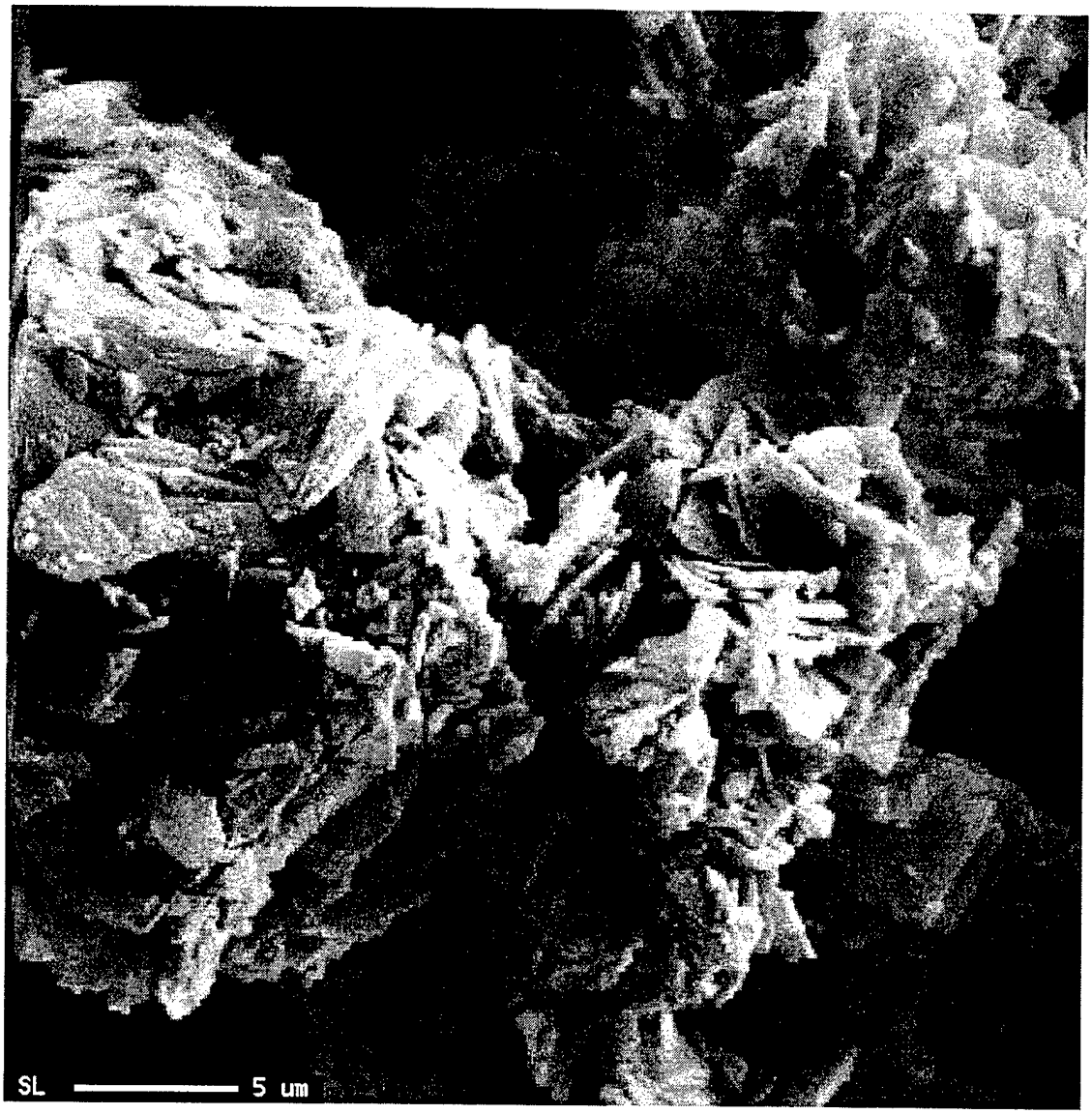

Figure 1a. SEM image of compound A.

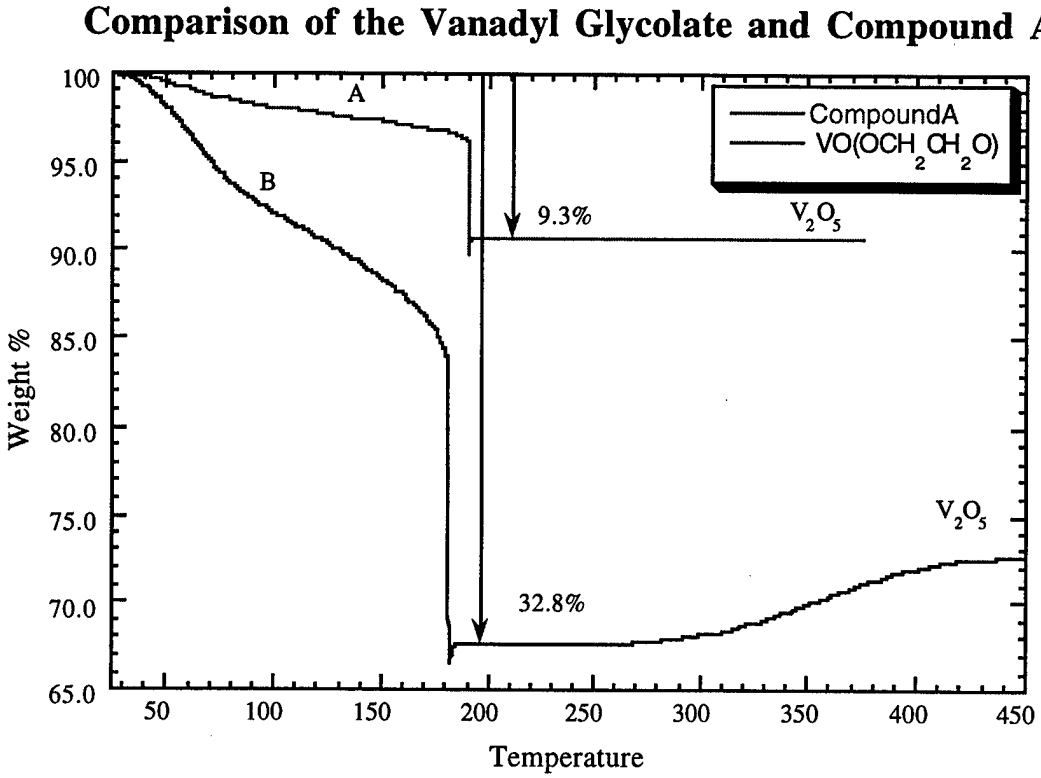

Figure2a. A comparison of the TGA plots for the two ethylene glycol based compounds.

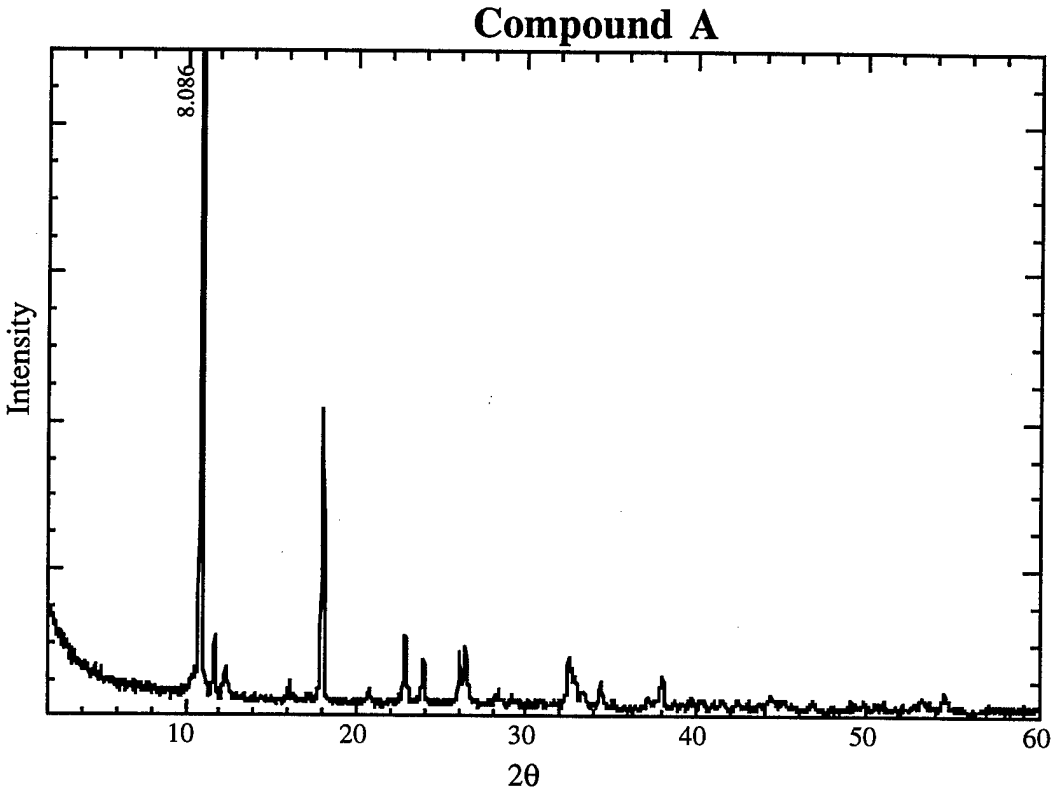

Figure3a. The powder X-ray diffraction pattern of compound A.

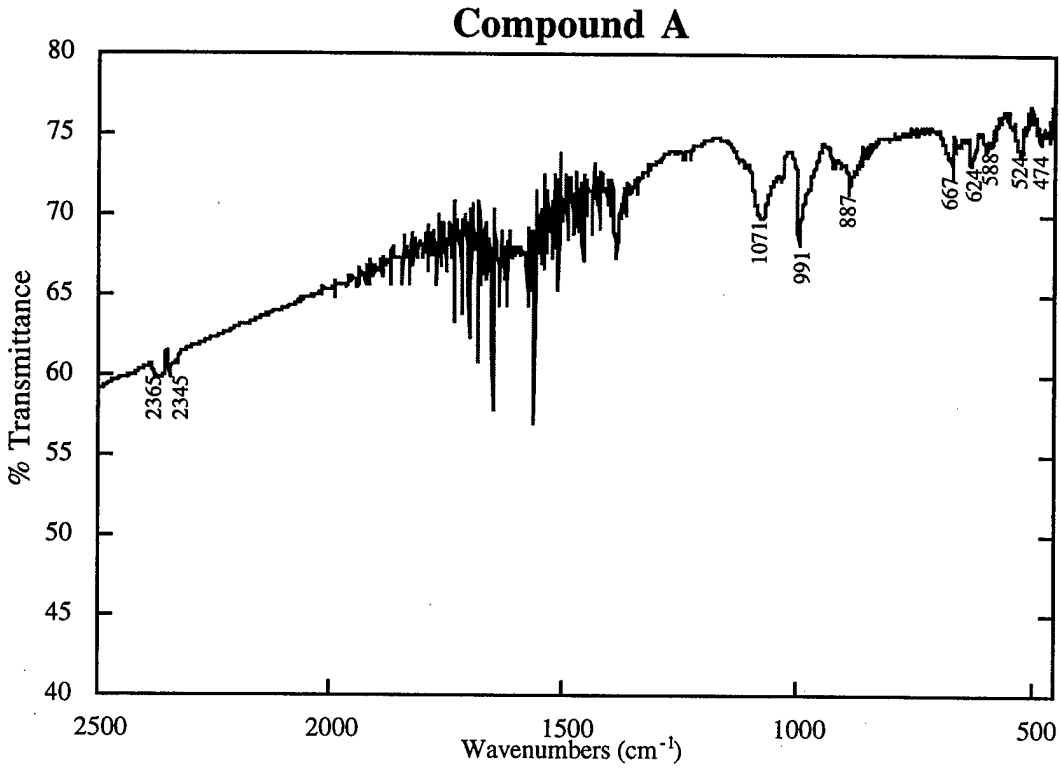

Figure 4a. The FTIR spectrum for compound A.

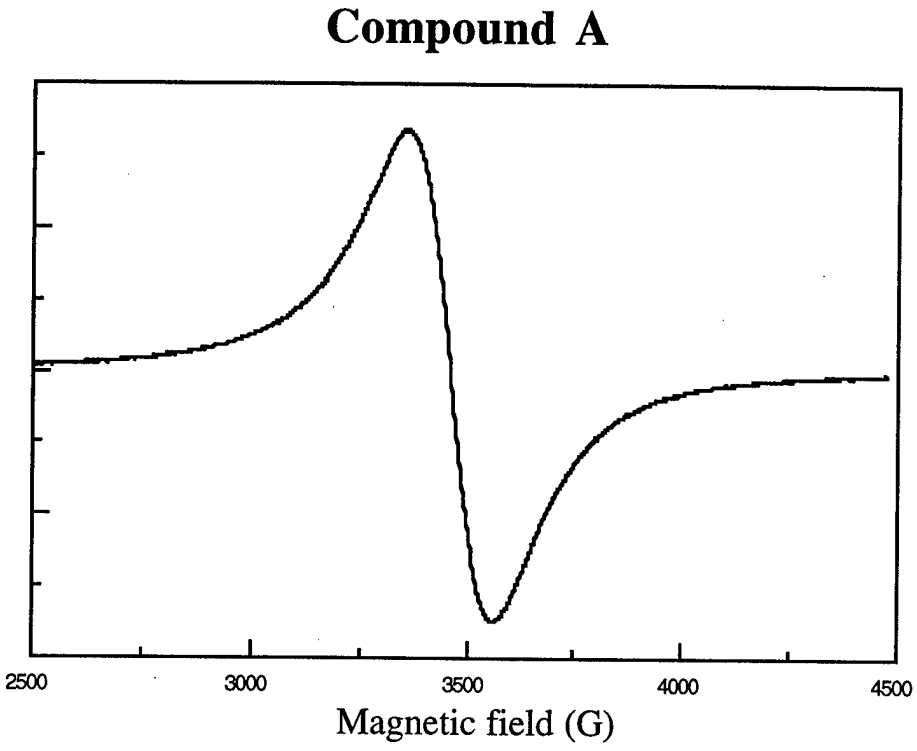

Figure 5. The EPR results for compound A.

THE E MATERIAL

Material E's dark colors of blue and black suggested a partial reduction of V^{+4} to V^{+5} of the vanadium atoms. The sample preparation for this material was similar to that of the trivanadium oxide hydrate except for the pH of the reaction mixture. Thus, the E material, had a lower pH because of the presence of additional acetic acid. The material was shown to have plate like features in the SEM images. (Figure 1e.)

The thermalgravimetric data showed there to be a similar weight loss curve as that of the F compound. The plot is shown in figure 2e. It lost a total of greater than 5% of its original weight upon heating under oxygen.

The XRD pattern of the material showed an extremely crystalline material with what appeared to be layers in the 00l direction. See figure 3e. The sample has been investigated with powder diffraction several times. The material's pattern showed a high crystallinity of the material, and an indexing of high merit is anticipated. With that, the structure would likely be solved and the material fully characterized. The material has been indexed, but not with a high enough certainty to publish. The material's strong 001, 002, 003... peaks were evident in the pattern. The FTIR spectrum of the material is shown in figure 4e.

The magnetic properties were explored using EPR spectroscopy. The g-factor was 1.955 for the E material, with moderately wide line width of 131 Gauss. See figure 5e.

Figure 1e. SEM image of compound E.

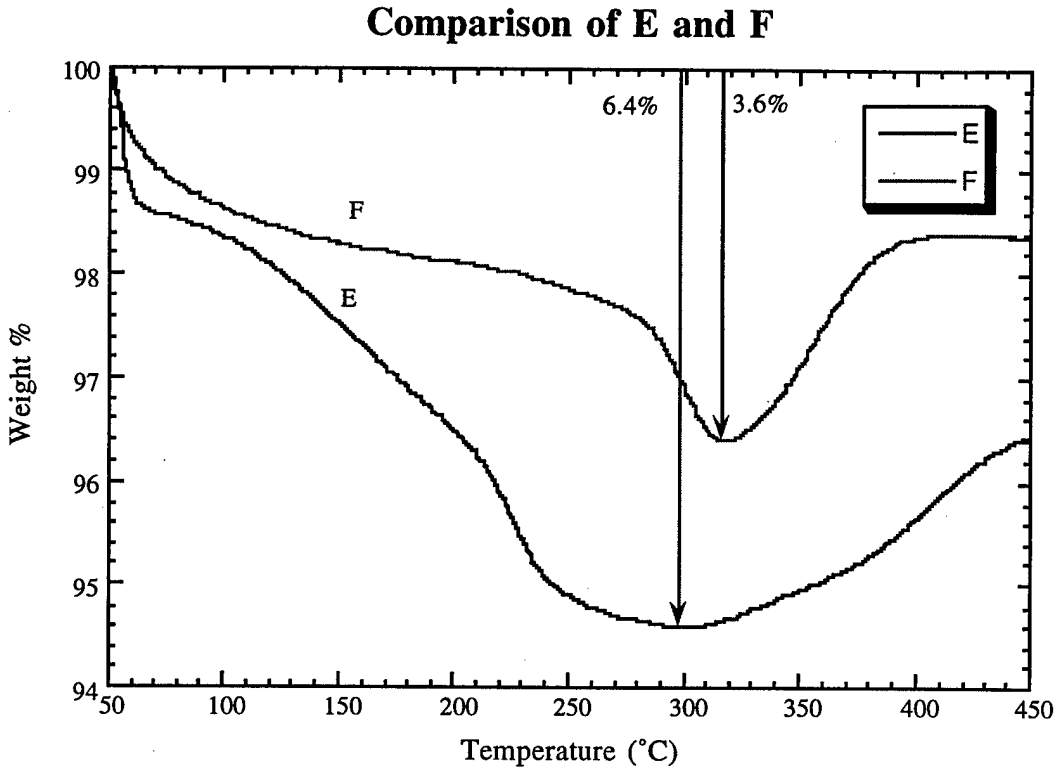

Figure 2e. Thermalgravimetric data for compound E.

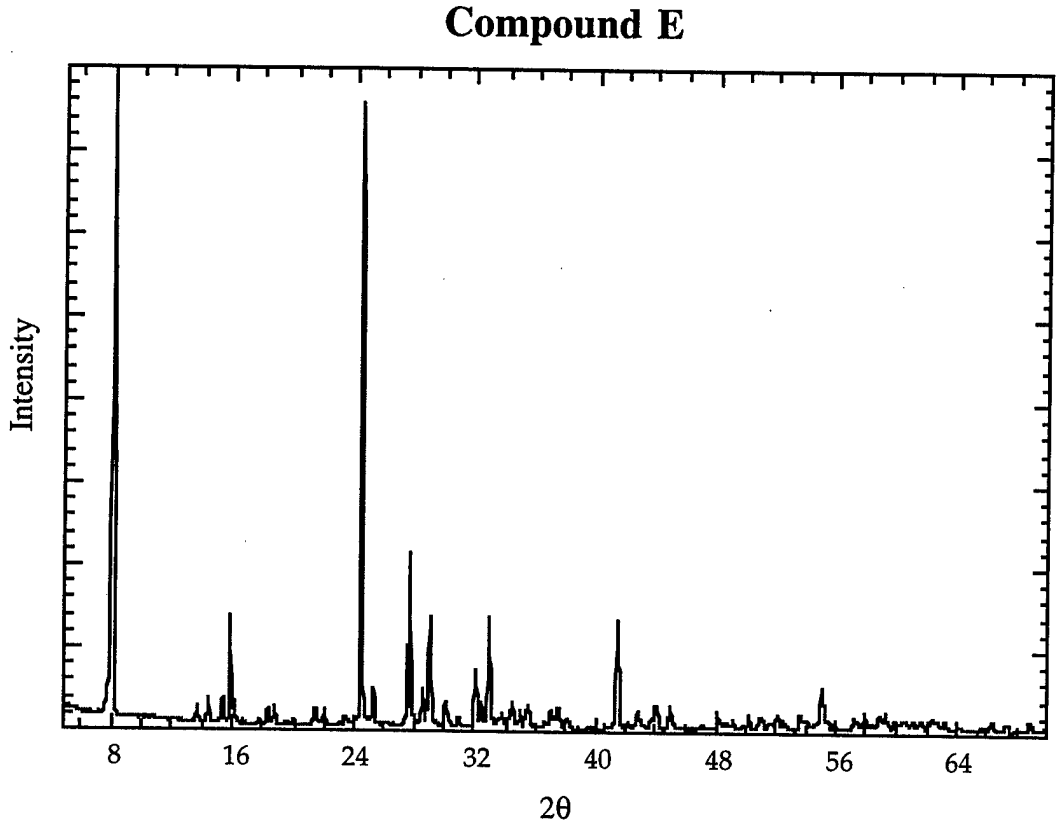

Figure 3e. The powder diffraction pattern of compound E.

Figure 4e. The FTIR spectrum.

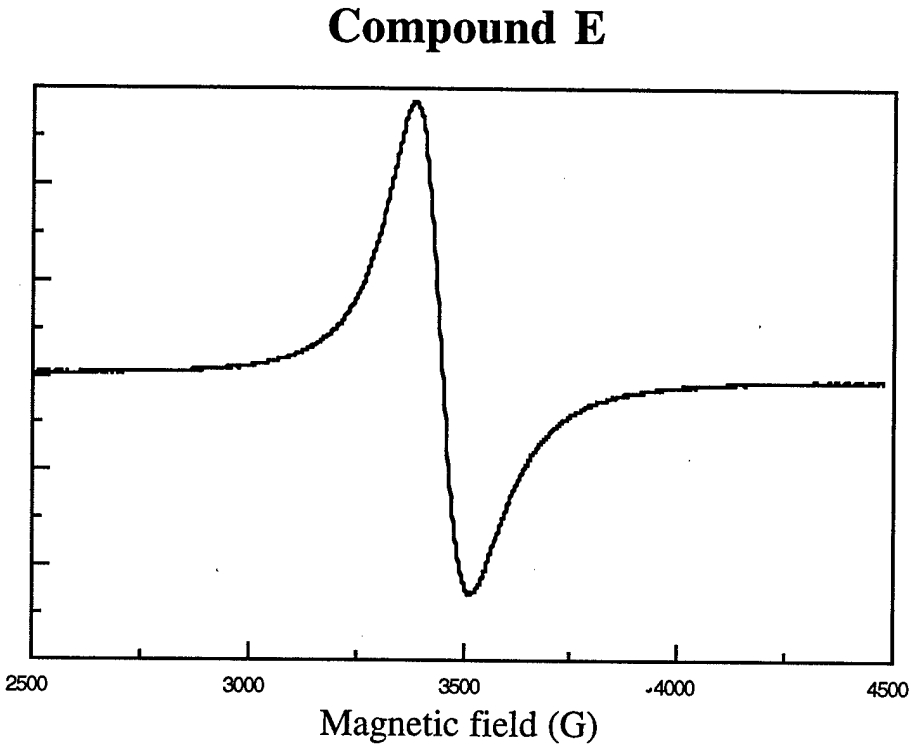

Figure 5e. The EPR results for compound E.

Chapter V - Summary

The efforts made in this study have been for two purposes. The first was to explore the impact of templating cations in the reaction medium of hydrothermal synthesis. The second was to investigate the use of some organic solvents such as ethylene glycol and acetic acid in the production of vanadium oxides. In most hydrothermal reactions, the solution mixture is aqueous based, but here water was only present to dilute the acid.

The organic solvents, acetic acid and ethylene glycol, were used because it was thought that they could replace the role of the organic cations discussed earlier. The organic cations, though structurally supportive, inhibited lithium insertion in electrochemical reactions. It was thought that the organic solvents of this study could bee structure supporting while neither occupying interlayer sites nor inhibiting the intercalation of the lithium.

The organic solvents, with their two accessible oxygen atoms, offered the bridging that was sought, but it occurred in the chains of the compounds made as opposed to in an interlayer support. The two chelating ligands of (CH_3COO) and (OCH_2CH_2O) did such in the vanadyl acetate and vanadyl glycolate compounds respectively. The materials were chain like with little interlayer attraction. A third material was made in the presence of the organic solvent. Though the structure has not yet been solved, it is shown to be flaky in nature in the SEM images.

The water diluted acetic acid mixtures led to the formation of two layered compounds. The $V_3O_7(OH_2)$ precipitated out of the solution of higher pH. With its existence known, this study offers a lower temperature method of preparation. The more acidic mixture produced a plate like material. The structure has not yet been solved, but is in progress. Theses two layered compounds offered support that organic cations are not needed to synthesize layered vanadium oxides.

The investigation concludes by reiterating what was accomplished and learned by the research group . Organic cations, which often lead to layered vanadium oxides, are not critical to their formation. The use of non aqueous solutions yielded one dimensional chain like structures. The dilute acid mixtures produced layered materials.

The two materials that were not completely characterized will continue to be explored by researchers in the materials group. They are new vanadium oxides with interesting topographical features.

References

1. Composites at Lake Louise (1997).

2. M.S. Whittingham, R. Chen, T. Chirayil and P. Zavalij, Solid State Ionics 94 (1997) 227.

3. L.H Gaines 11th. Intersociety Energy Conversion 1976.

4. M. S. Whittingham and Fred Gamble Jr, Mat. Res. Bull. 10 (1975) 363.

5. M. Dines, Mat. Res. Bull. 10 (1975) 287.

6. R.B. Somoano, V. Hadek and A. Rembaum, 58 (1973) 697.

7. A. LeBlanc M. Danot and J. Rouxel, Bull. Soc. Chim. Fr. 87 (1969)

8. A. LeBlanc and J. Rouxel, Compt. Rend. 247C (1972) 786.

9. T.L. Brown and H.E. LeMay, Chemistry the Central Science, Prentice Hall (1985).

10. D. Guyomard nad J.M. Tarascon, J. Electrochem. Soc. 139 (1992) 937.

11. F. Leroux, D. Guyomard and Y. Piffard, Solid State Ionics 80 (1995) 307.

12. J.M. Tarascon, E. Wang, F.K. Shokoohi, W.R. McKinnon and S. Colson, J. Electrochem.Soc. 138 (1991) 2859.

13. G. Pistoia, Lithium Batteries: New Materials Developments and Perspectives, Elsever Science (1994).

14. A. Bystrom, K. A. Wilhelmi and O. Brotzen, Acta Chem. Scand. 14 (1950) 1119.

15. E. Gillis and E. Boesman, Phys. Status, Solidi. 14 (1966) 337.

16 B. Pecquenard, D. Gourier and N. Baffin, Solid State Ionics 78 (1995) 287.

17. C.D. Tuck, Modern Battery Technology Ellis Horwood (1991).

18. G. Sperlich, Z. Physik 250 (1972) 335.

19. C. Sanchez, M. Henry, R. Morineau, and M.C. Leroy, Phys. Status Solidi.(b) 122 (1984) 175.

20. J. Livage, C. Sanchez and J. Vedal, Solid State Ionics 1 (1980) 491.

21. D. W. Murphy, P.A. Christian, F. J. DiSalvo and J.V. Waszczak, Inorg. Chem. 18 (1979) 2800.

22. J.M. Cocciantelli, J.P. Doumerc, M. Pouchard, M. Broussely and J. Labat, J. Power Sources 34 (1991) 103.

23. R.M. Barrer Hydrothermal Chemistry of Zeolites, Academic Press London (1992).

24. J.S. Beck, J.C. Vartuli, W.J. Roth, M.E. Leonowicz, C. T. Kreseg, K.D. Schmitt, C. T-W. Chu, D.H. Olson, E. W. Sheppard, S. B. McCullen, J.B. Higgins and J. Schlenker, J. Am. Chem. Soc. 114 (1992) 10843.

25. J.W. Johnson, A.J. Johnson, A.J. Jacobson, J.F. Brody and J. M. Rich, Inorg. Chem. 21 (1982) 3800.

26. R.C. Haushaulter, K.G. Strohmailer and F.W. Lai, Science 246 (1989).

27. M.S. Whittingham, Current Opinions in Solid State and Material Scinece 1 (1996) 227.

28. T.G. Chirayil, P.Y. Zavalij and M.S. Whittingham, J. Electrochem. Soc. 143 (1996) 193.

29. A.K. Cheetham and P. Day, Solid State Chemistry: Techniques Oxford Press (1990).

30. F. Theobald and R. Cabala, C.R> Acad. Sci. Ser. C 200 (1970) 26.

31. S. Komarneni, Q.H. Li and R. Roy, J. Mat. Chem. 4 (1994) 1903.

32. I. Girnus, M.M. Pohl, J, Richter-Mendau, M. Schneider, M. Noack, D. Venzke and J. Caro, Advanced Mater. 7 (1995) 29.

33. T.G. Chirayil, P.Y. Zavalij and M.S. Whittingham, Chem. Comm. 33 (1997).

34. T.G. Chirayil, P.Y. Zavalij and M.S. Whittingham, J. Mat. Chem. 11 (1997) 2193.

35. T.G. Chirayil, P.Y. Zavalij and M.S. Whittingham, Solid State Ionics 84 (1996) 163.

36. P.Y. Zavalij, M.S. Whittingham, E.A. Boyle, V.K. Pecharsky, and R.A. Jacobson, Z. Krist. 211 (1996) 464.

37. V.W. Day, W.G. Klepmerer, and O.M. Yaghi, J. Am. Chem. Soc. 111 (1989) 5959.

38. O. Odunola, Ghana J. Chem. 1 (1995) 461.

39. R.T. Morrison and R.N. Boyd, Organic Chemistry Prentice Hall (1992).

40. O.Y. Yao and T. Yamamoto, J. Solid State Chem. 89 (1990) 372.

41. C. Pouchert, Aldrich Library of Infrared Spectra (1981).